A Tribute to Michael R. Raupach for Contributions to Aeolian Fluid Dynamics

Yaping Shao[1], William Nickling[2], Gilles Bergametti[3], Adrian Chappell[4], Paul Findlater[5], Jack Gillies[6], Masahide Ishizuka[7], Martina Klose[1], Jasper Kok[8], John Leys[9], Hua Lu[10], Beatrice Marticorena[3], Grant McTainsh[11], Cheryl McKenna-Neuman[12], Gregory S. Okin[13], Craig Strong[14], Nicholas Webb[15]

[1]Institute for Geophysics and Meteorology, University of Cologne, Cologne, Germany; yshao@uni-koeln.de; mklose@uni-koeln.de
[2]Department of Geography, University of Guelph, Ontario, Canada; nickling@uoguelph.ca
[3]Laboratoire Interuniversitaire des Systèmes Atmosphériques, Universités Paris Diderot and Paris Est, France; Gilles.Bergametti@lisa.u-pec.fr; Beatrice.Marticorena@lisa.u-pec.fr
[4]CSIRO, Division of Soil and Landscape Science, Canberra, Australia; Adrian.Chappell@csiro.au
[5]WA Department of Agriculture and Food, Geraldton, Australia; paul.findlater@agric.wa.gov.au
[6]Desert Research Institute, USA; Jack.Gillies@dri.edu
[7]Faculty of Engineering, Kagawa University, Japan; ishizuka@eng.kagawa-u.ac.jp
[8]Department of Atmospheric and Oceanic Sciences, University of California, Los Angeles, USA; jfkok@ucla.edu
[9]NSW Office of Environment and Heritage, Gunnedah, Australia; John.Leys@environment.nsw.gov.au
[10]British Antarctic Survey, Cambridge, UK; hlu@bas.ac.uk
[11]Griffith School of Environment, Griffith University, Australia; g.mctainsh@griffith.edu.au
[12]Department of Geography, Trent University, Ontario, Canada; cmckneuman@trentu.ca
[13]Department of Geography, University of California, Los Angeles, USA; okin@ucla.edu
[14]Australian National University, Canberra, Australia; craig.strong@anu.edu.au
[15]USDA-ARS Jornada Experimental Range, Las Cruces, USA; nwebb@nmsu.edu

Aeolian Research

Abstract: Since the pioneering work of Bagnold in the 1940s, aeolian research has grown to become an integral part of earth-system science. Many individuals have contributed to this development, and Dr. Michael R. Raupach (1950 - 2015) has played a pivotal role. Raupach worked intensively on wind erosion problems for about a decade (1985 - 1995), during which time he applied his deep knowledge of turbulence to aeolian research problems and made profound contributions with far-reaching impact. The beauty of Raupach's work lies in his clear conceptual thinking and his ability to reduce complex problems to their bare essentials. The results of his work are fundamentally important and have many practical applications. In this review we reflect on Raupach's contribution to a number of important aspects of aeolian research, summarize developments since his inspirational work and place Raupach's efforts in the context of aeolian science. We also demonstrate how Raupach's work provided a foundation for new developments in aeolian research. In this tribute, we concentrate on five areas of research: (1) drag partition theory; (2) saltation roughness length; (3) saltation bombardment; (4) threshold friction velocity and (5) the carbon cycle.

1. Introduction

Aeolian research is multi-disciplinary, but its core lies arguably in the fluid dynamic interactions between soil particles, the atmosphere, and the soil surface. Since the early work of Bagnold (1941), it has advanced to become an integral part of earth-system studies. Aeolian processes are highly relevant topics in the earth sciences because of the need to: (1) better quantify the dust cycle for climate projections; (2) assess the anthropogenic impact on natural and human environments; (3) prevent soil loss from wind erosion in land-conservation practice; and 4) understand aeolian processes and landform development on other planets in particular, Mars and Venus, as well as moons such as Titan. Many individuals have contributed to this development, and Dr. Michael R. Raupach (1950 – 2015) was one of the most outstanding (Steffen, 2015).

For colleagues in aeolian research, and in climate research at large, Michael R. Raupach is Mike, but he used to abbreviate his name MR^2, a format that we shall adopt in this paper. This abbreviation was related to his university training in Applied Mathematics. MR^2 received his BSc degree, with honors in mathematical physics, from the University of Adelaide in 1971, and a PhD in micrometeorology (under the supervision of Prof. Peter Schwerdtfeger) from the Flinders University of South Australia in 1976. After a postdoctoral position at the University of Edinburgh, he joined the Centre for Environmental Mechanics (CEM, also referred to as the Pye Lab) of the CSIRO (Commonwealth Scientific and Industrial Research Organisation) in Canberra in 1979, where he worked for much of his 35-year career. From 2000 to 2008, he was inaugural co-chair of the Global Carbon Project, an international program bridging the research effort between the natural and human dimensions of the carbon cycle. In February 2014, he took up the role of Director at the Climate Change Institute of the Australian National University and remained an Honorary Fellow with the CSIRO. Based on his research foci, his career can be divided into two stages. In the first he worked on atmospheric boundary-layer turbulence and atmosphere-land-surface exchanges, including aeolian processes, and in the second on climate change, in particular the carbon cycle.

Raupach's scientific drive originated from his passion for protecting the environment, and his interest in aeolian processes following from his concerns with land conservation. The period of 1977 – 1988 saw three successive El Niño events, including the intense phase of 1982 – 1983, which brought record drought to eastern Australia, turning the farmlands in the wheat-sheep belt into a hot spot of wind erosion. On 8 February 1983, a "cool change" (a dry cold front) preceded by hot (43.2ºC) gusty northerly winds blew large quantities of red-brown dust over Melbourne. This event inspired MR^2 to write one of his first essays on wind erosion (Raupach et al., 1994), which was pioneering in its attention to three fundamental goals of dust research: identification of dust sources; estimating dust loads; and quantifying the nutrient loss of topsoil by wind erosion. Their estimate of the dust loading (2 ±1 Mt) in the 1983 Melbourne dust storm was one of the earliest attempts to quantify event-based dust loading. This value was based upon a few back-of-the-envelope calculations; reducing a complex problem to its fundamental components, for which MR^2 became famous. Raupach's estimate of topsoil nutrient loss was highly innovative, and 20 years later, wind-erosion related soil nutrient and soil carbon transport has become one of the most fundamental aspects of studies on the dust cycle.

In 1985, John Leys, then with the New South Wales Soil Conservation Service, had just started his PhD at Griffith University in Brisbane under the supervision of Professor Grant McTainsh, and was developing a portable wind tunnel for wind-erosion field experiments. At the time, MR^2 was among a group of world-class micro-meteorologists gathered in the Pye Lab, conducting wind-tunnel experiments on flow over complex terrains. MR^2 and Leys went on to modify the design of Marsh and Carter (1983) and develop Australia's aeolian-research wind tunnel (Leys and Raupach, 1990). The excellent fluid dynamic features of this tunnel made it a valuable research tool not only for land-conservation studies (McTainsh and Leys, 1993), but also for the studies of basic wind-erosion processes (Shao and Raupach, 1992; Shao et al., 1993). In 1991, a group of Australian wind-erosion researchers gathered at the Murdoch University in Perth and staged the 1st Australian workshop on wind erosion (Figure 1). In this workshop, William Nickling gave a keynote presentation "Shear Stress: What Drives Wind Erosion Processes". Following the meeting, with a cool sea breeze and bright stars in the sky in the port of Freemantle, MR^2 treated everyone with beer. In 1993, the group met again in the Mallee country town of Mildura and formed the Wind Erosion Research Community of Australia (WERCA, a name that MR^2 and Grant McTainsh conceived over drinks at the meeting). Dale Gillette gave a philosophical talk on the paradigms of wind erosion. It is unfortunate that MR^2 will not be with us for the ninth International Conference on Aeolian Research (ICAR IX) to be held in Mildura in 2016. However, the influences of his work will be evident at the conference and will provide a legacy for a considerable time.

[Insert Figure 1 here]

Figure 1: Michael R. Raupach (back, 6th left) among the participants of the 1st Australian Workshop on Wind Erosion, 1991, Murdoch University, Perth. Several contributors to this paper were among the participants: Grant McTainsh (front, 1st left), Paul Findlater (front, 2nd left), Yaping Shao (back, 1st left), William Nickling (back, 5th left), John Leys (back, 7th left). The workshop convener was William Scott (front, 3rd left).

MR^2 worked for about a decade (1985 – 1995) intensively on wind erosion problems, but he did so brilliantly by relating aeolian problems to his deep knowledge of turbulence, and made profound contributions to the field with far-reaching influences and a lasting legacy. The beauty of Raupach's work is crystal clear conceptual thinking, reducing problems to their essentials and expressing that essence with elegance yet simplicity. The results of his work are robust and practically applicable. In this review we reflect on Raupach's contribution to a number of important aeolian research themes, summarize the developments since his inspirational work and place Raupach's effort in the context of aeolian science. We also demonstrate how Raupach's work provided many foundations or platforms for the development of his work and the investigation of new research. For brevity, we will concentrate on Raupach's work in five areas: (1) drag partition theory; (2) saltation roughness length; (3) saltation bombardment; (4) threshold friction velocity; and (5) carbon cycle.

2: Drag Partition Theory and Applications to Wind Erosion Studies

2.1 The Raupach Drag Partition Theory

In the atmospheric surface layer, the profile of the mean wind is approximately logarithmic in form and the shear stress, τ, also referred to as drag, is vertically approximately constant. Thus, the flow in the surface layer is characterized by the aerodynamic roughness length, z_0, and the shear stress that is often expressed in terms of friction velocity, $u_* = \sqrt{\tau / \rho}$, with ρ being air density.

At the second International Conference on Aeolian Research (ICAR II) in Denmark (1990), MR^2, Gillette and Leys discussed the difficulties of sand flux modelling in the shrub lands of Texas and Australia as opposed to the sandy beaches of Denmark. They soon realized that in many wind-erosion applications, the knowledge of τ alone is insufficient, as in shrub lands the shear stress on the intervening erodible surface, which drives the sand movement, is subject to the influences of the shrubs. MR^2 generalized this discussion to the fluid dynamic problem of drag partition over rough surfaces, i.e., the partition of the total drag into a pressure drag on roughness elements and a friction drag on the surface. Raupach (1992) laid the foundation of the drag partition theory and Raupach et al. (1993) demonstrated how this theory can be applied to estimating sediment transport threshold over various rough aeolian surfaces. Raupach's work led the way to numerous studies that followed, ranging from wind-tunnel and field experiments, numerical modelling, remote sensing and theory. We know today that it is desirable in general to treat τ in wind erosion applications as a stochastic variable and to statistically quantify its spatial and temporal variations. As discussed later in this review, the spatial variability of shear stress is a critical part of heterogeneous aeolian processes, while its temporal variability is important for intermittent saltation and dust emission.

Shear stress variation in nature can be very complicated, and simplifications are necessary for theoretical analysis (Lettau, 1969; Arya, 1975). Following Schlichting (1936), Raupach (1992) suggested that a rough surface can be considered to be composed of roughness elements (in the spirit of Raupach's analysis, it seems appropriate to invent the word "roughtons") superposed on a smooth substrate surface. The total drag is thus expressed as:

$$\tau = \tau_r + \tau_s \qquad (1)$$

where τ_r is the drag on the roughtons, or pressure drag, and τ_s the drag on the substrate surface, or surface drag. The task of drag partition is to determine the ratios τ_r / τ and τ_s / τ, and to estimate how these ratios depend on the roughness characteristics. An immediate question that arises is how the surface roughness can be quantified. MR^2 aimed to find an analytical solution for the simplest case possible and thus assumed that the surface consists of randomly distributed cylinders uniform in size, each having a frontal area of a_f. It follows that if the number density of the roughtons is n (number per unit area), then the frontal area index of the roughtons is

$$\lambda = n \cdot a_f \qquad (2)$$

which is the only input parameter for the Raupach (1992) scheme. This conceptual simplification was influenced by the work MR^2 was very familiar with, in particular the wind-tunnel experiments of Marshall (1971) and Wooding et al. (1973), all from the Pye Lab.

Raupach (1992) introduced the concept of effective shelter area, A, and volume, V, associated with an individual roughton (Figure 2), and made two hypotheses:

Hypothesis I: for an isolated roughness element of breadth b and height h in a deep turbulent boundary layer with friction velocity u_* and mean velocity U_h at height h the effective shelter area A and volume V scale as:

$$A \sim bhU_h / u_* \tag{3a}$$

$$V \sim bh^2 U_h / u_* \tag{3b}$$

Hypothesis II: when roughness elements are distributed uniformly or randomly across a surface, the combined effective shelter area or volume can be calculated by randomly superposing individual shelter areas or volumes.

With these hypotheses, Raupach (1992) found that

$$\frac{\tau_s}{\tau} = \frac{1}{1+\beta\lambda} \tag{4a}$$

$$\frac{\tau_r}{\tau} = \frac{\beta}{1+\beta\lambda} \tag{4b}$$

with $\beta = C_r / C_s$, where C_s is the frictional drag coefficient and C_r the pressure drag coefficient. Eq. (4) is a simple yet robust model supported by the wind-tunnel measurements of Marshall (1971) as well as the numerical simulations of Li and Shao (2003).

[Insert Figure 2 here]

Figure 2: Raupach's conceptual model for drag partitioning. A rough surface is considered to consist of roughness elements and a substrate surface. A roughness element produces an effective sheltering area and volume. The integrative effect of the roughness elements can be estimated by random superposition [Redrawn from Raupach (1992)).

The results of Raupach (1992) have two immediate applications, first to estimate threshold friction velocity for wind erosion, u_{*t}, and second to estimate aerodynamic roughness length, z_0. Suppose for a surface σ is the ratio of roughton basal area to frontal area, then the exposed fraction of the surface subject to wind erosion is $(1-\sigma\lambda)$, and the shear stress on the exposed surface is:

$$\frac{\tau'_s}{\tau} = \frac{1}{(1-\sigma\lambda)}\frac{1}{(1+\beta\lambda)} \tag{5}$$

Here, τ'_s is the spatially averaged stress on the exposed surface. If we assume the largest stress acting on the surface is τ''_s and $\tau''_s(\lambda)$ equals $\tau'_s(\lambda_0)$ with $\lambda_0 = m\lambda$ and $m<1$, then we have:

$$R_t^2 \equiv \frac{\tau''_s}{\tau} = \frac{1}{(1-m\sigma\lambda)}\frac{1}{(1+m\beta\lambda)} \tag{6}$$

R_t is the ratio of u_{*ts}/u_{*tr}, with u_{*ts} being the threshold friction velocity for the surface free of roughtons and u_{*tr} for the rough surface. It follows that:

$$u_{*tr} = u_{*ts}\sqrt{(1-m\sigma\lambda)(1+m\beta\lambda)} \qquad (7)$$

Equation (7) provides a simple way for the correction of u_{*t} for rough surfaces, and its validity is confirmed through comparison with the existing data of Gillette and Stockton (1989), Musick and Gillette (1990), Lyles and Allison (1976), Iversen et al. (1991), Crawley and Nickling (2003), Li and Shao (2003), and Sutton and McKenna-Neuman (2008).

Raupach (1992) and Raupach et al. (1993) provided for the first time a strong theoretical underpinning for explaining the impacts of roughness elements on aeolian thresholds and fluxes and a deep insight into the aeolian fluid dynamics. The method used in Raupach (1992) is unique in that by introducing the sheltering area and volume, MR^2 took a "quantum fluid" approach, in that he discretely quantified the effect of an individual roughness element and then estimated the total effect of all roughness elements through random superposition. For this reason, it is appropriate to call roughness elements roughtons.

2.2 Wind-tunnel and Field Experiments on Drag Partition

To test the theory of Raupach (1992) and Raupach et al. (1993), William Nickling and Jack Gillies thought it critical to: (1) bridge theory to field measurements at the full scale; (2) examine how R_t behaves if roughness elements are real plants; and (3) investigate the impact of roughness elements on saltation transport, in addition to mean u_{*t}. They carried out field and wind-tunnel studies to evaluate C_r as a function of the Reynolds number, R_e, for different plants (Gillies et al., 2000; 2002). At the USDA Jornada Experimental Range (Gillies et al., 2006; 2007), they placed staggered arrays of large cylindrical roughness elements on a bare open surface and instruments between them to measure the total drag, surface drag, pressure drag and sand fluxes. It was found that C_r for plants is both plant-form and R_e dependent. This implies that drag partition for surfaces with plants is not necessarily fixed, but changes as the plants reconfigure themselves in response to wind. The more flexible the plant, the greater the proportion of shear stress acting on the substrate surface, and C_r declines with R_e. This finding implies that steppe landscapes (Shinoda et al., 2011), which are typically composed of grass-type species, are likely more erodible than the shrub-dominated landscapes of the southwestern US deserts (Gillette and Pitchford, 2004; Gillette et al., 2006; King et al., 2005). It was also found that while sand flux scales with λ, it is also dependent on the height of the roughtons. For the same λ, elements with $h \geq 0.3$ m are more effective in reducing sand flux than shorter elements, e.g., $h \leq 0.1$m (Gillies et al., 2006; Gillies and Lancaster, 2013; Gillies et al., 2015). These experiments show that the Raupach et al. (1993) model performs well in general, but additional considerations should be given to roughness configuration to fully account for the observed saltation flux variations over rough surfaces. While Eq. (7) has three parameters, m, σ and β, it appears sufficient to choose appropriate β values (between 100 and 400) to fully describe the observed R_t for a wide range of surfaces, but to keep m and σ constant [e.g. 0.5 and 1, respectively, as set Raupach et al. (1993))), as Figure 3 shows.

[Insert Figure 3 here]

Figure 3: A compilation of R_t versus λ data from wind-tunnel and field experiments (symbols). RGL93_1, RGL93_2 and RGL93_3 are the estimates using the Raupach et al. (1993) scheme with m = 0.5, σ = 1, and β = 100, 200 and 400, respectively.

The simplicity of Eq. (7) is a strength for its application, in that it requires only a few measurable parameters (Wolfe and Nickling, 1996; Lancaster and Baas, 1998; King et al., 2006). This approach is widely used today in wind erosion models. In some studies e.g., Marticorena and Bergametti (1995), the drag partition scheme of Arya (1975) based on roughness length is used. However, because roughness length is closely related to roughness configuration (e.g., frontal area index, λ), the schemes of Arya (1975) and Raupach (1992) and Raupach et al. (1993) are in essence equivalent (see also, Raupach, 1994).

2.3 Extension of Drag Partition Theory

Real aeolian surfaces are much more complex than is assumed in Raupach (1992) and Raupach et al. (1993). For practical applications, the Raupach (1992) theory requires several extensions: (1) the validity of Eq. (4) is limited to about $\lambda \le 0.1$, but natural surfaces often have much larger roughness densities; (2) for surfaces with larger λ, it is not clear how shelter areas and volumes can be evaluated and how they superpose due to the interactions among the turbulent wakes associated with the roughness elements; (3) there are large uncertainties in the parameters β and *m*, as both are dependent on the roughness-element properties (e.g., porosity and elasticity) and configuration (arrangement and aspect ratio).

It is possible to derive the results of Raupach (1992) with simpler assumptions. For instance, it is sufficient to assume linear superposition of shelter areas and volumes instead of random superposition as applied in Raupach (1992) (Shao and Yang, 2008). More generally, we can write

$$\tau_s = \rho f_s C_s U_h^2 \qquad (8a)$$

$$\tau_r = \rho f_r C_r \lambda U_h^2 \qquad (8b)$$

where f_r and f_s are modification functions of the respective drag coefficients arising from the interacting flows shed by roughtons. Equation (8) leads to Eq. (4), subject only to $f_s = f_r$, which is $\exp(-c\lambda U_h / u_*)$ in Raupach (1992).

Equation (1) is appropriate for small roughness density, but as λ increases, the total drag on the rough surface, τ, is better written as:

$$\tau = \tau_r + \tau_s + \tau_c \qquad (9)$$

where τ_c is the friction drag on the surfaces of roughness elements. As $\lambda \to \infty$, we expect $\tau_r / \tau \to 0$ but Eq. (4) states that $\tau_r / \tau \to 1$ due to the neglect of τ_c. In general, the total drag can be partitioned into three components following Eq. (9) and the individual terms expressed as:

$$\tau_r = \rho f_r C_r \lambda U_h^2 (1-\eta) \qquad (10a)$$

$$\tau_s = \rho f_s C_s U_h^2 (1-\eta) \qquad (10b)$$

$$\tau_c = \rho C_s U_h^2 \eta \qquad (10c)$$

where η is fraction of cover and f_r and f_s are functions of λ and η represent the modifications to C_r and C_s arising from the interactions of the turbulent wakes of roughness elements. With this formulation, the drag partition problem is now reduced to determine f_r and f_s. It is also found in Shao and Yang (2008) that

$$\frac{u_*^2}{U_h^{\ 2}} = f_r \lambda (1-\eta) C_r + [f_s (1-\eta) + \eta] C_s \qquad (11)$$

that shows that u_*^2/U_h^2 is a weighted average of the pressure and surface drag coefficients. In neutral atmospheric boundary layers, we have $U_h = \frac{u_*}{\kappa} \ln\left(\frac{h-d}{z_0}\right)$ and Eq. (11) can be written as:

$$\kappa^2 \ln^{-2}\left(\frac{h-d}{z_0}\right) = f_r \lambda (1-\eta) C_r + [f_s (1-\eta) + \eta] C_s \qquad (12)$$

Equation (12) shows that the roughness length, z_0, can be determined in terms of drag coefficients for a given zero-displacement height, d. Thus, in a drag partition theory, we actually make two inter-related statements. The first is about the behavior of drag partition functions; and the second about the behavior of u_*/U_h or equivalently a statement on the drag coefficients or on the roughness length, z_0. The above formulation of Shao and Yang (2008) as an extension of Raupach (1992) reduces the drag partition problem to the determination of the drag coefficients modification functions. The Shao and Yang scheme requires both frontal area index and fraction of cover as input parameters.

Another extension of Raupach (1992) was made by Okin (2008). The Okin scheme builds on the basic insight that τ_s in the lee of a roughton increases with distance downwind. While Raupach (1992) expressed the wake effect by means of shelter area and volume, the Okin scheme takes a probabilistic approach that envisions the surface to be made up of points that are some distance downwind of a roughton. The shear stress experienced at each point is an increasing function of this distance, scaled by the height of the roughton, multiplied by τ. With this approach, the frontal area index is no longer the best variable for characterizing vegetation cover, but is replaced by the separation distance between the roughtons. In Okin (2008), the shear stress on the soil surface is variable across the landscape, as originally envisioned in Raupach (1992). This approach allows some areas of the surface to experience transport while the more protected areas do not. This approach differs from that of Raupach et al. (1993) in which the threshold shear stress is seen to be a property of the bulk surface. As a result, the Okin scheme is able to predict transport even at relatively high vegetation cover, in accordance with field observations. Several studies published since have supported this approach (Webb et al., 2014; Walter et al., 2012a; 2012b; Li et al., 2013).

2.4 Saltation Heterogeneity

At ICAR-V (Lubbock, USA, 2002), MR^2 incisively exposed the challenges of large scale aeolian modelling. Raupach and Lu (2004) subsequently published a review of land surface processes on aeolian transport modelling during the previous two decades and identified four challenges: (1) the fidelity of process representation; (2) upscaling point-scale process models in the presence of unresolved heterogeneity in space and time; (3) availability of spatial data for specifying model inputs and boundary conditions; and (4) large-scale parameter estimation.

To date, these challenges remain largely unresolved but the explicit and clear articulations in Raupach and Lu (2004) provide essential guidance for what needs to be done.

Raupach and Lu (2004) suggested that improvements should be made in point-scale parameterisations including "…the effects of crusts and surface cohesion leading to supply-limited saltation and dust uplift, deposition to sparse vegetation…". There have been some developments in this area in particular with investigations of soil moisture (e.g., Wiggs et al., 2004), the use of laser scanning technology to describe small-scale roughness dynamics (e.g., Nield et al., 2013), angular reflectance measurement and bi-directional reflectance modelling to characterize changes in soil condition in space and time (Chappell et al., 2005; 2006; 2007) and retrieval of roughness changes in space and time using satellite remote sensing (Wu et al., 2009).

Raupach and Lu (2004) characterised point-scale transport models as, $f = f(v)$, where f is a flux and v is a vector of control variables. Part of the challenge with aeolian transport models is that they require flux and driving variables averaged in space and time. Raupach and Lu (2004) first defined

$$\bar{f}(\bar{v}) = \int f(v)p(v)dv \qquad (13)$$

where $p(v)$ is the probability density function (PDF) of v. If $f(v)$ is linear, then $\bar{f}(\bar{v})$ has the same form as $f(v)$. Raupach and Lu (2004) considered the cases when $f(v)$ is highly nonlinear (e.g., involving threshold responses), which originates from the interaction between the nonlinearity in $f(v)$ and statistical variability in v that causes the upscaling problem to be mathematically nontrivial and dependent on sub-grid-scale variability through the PDF $p(v)$. Raupach and Lu (2004) used an example of heterogeneous vegetation to show profoundly that "…major errors arise from upscaling procedures, which neglect the interaction between model nonlinearity and statistical variability in driving variables". They also demonstrated that even a first approximation to the sub-grid-scale variability can lead to substantial improvement in flux estimates.

The effect of surface heterogeneity, i.e., the deliberately neglected "level of details" in Raupach et al. (1993) has been subject to intensive studies in more recent years, as it has been identified as a significant source of uncertainty in its application. Yang and Shao (2005) demonstrated that in case of very small roughness density, the shear stress variability due to the presence of roughtons actually enhances rather than supresses wind erosion. Raupach and Lu (2004) recognised that while no sediment transport is predicted at large λ, this may happen in reality depending on roughness configuration (Okin, 2008), and that accounting for the PDF of λ can improve the model estimates, although this can be practically difficult (Walter et al., 2012; Dupont et al., 2013; 2014).

Brown et al. (2008) conducted wind-tunnel experiments to determine the PDF of τ_s and R_t for a range of λ, roughness configurations, and free-stream wind velocities, U_h. The authors demonstrated that the Raupach et al. (1993) scheme captures the general behaviour of R_t, but to accurately reproduce R_t, both β and m must be tuned for each case. Furthermore, the Raupach et al. (1993) scheme does not accurately reproduce R_t unless β is made variable to suit the roughness configurations (Walter et al., 2012a). This variability is illustrated as the scatter seen in Figure 3.

Webb et al. (2014) explored the effect of roughness configuration on sediment flux, Q, by comparing Q predicted using the Raupach et al. (1993) scheme using the τ_s PDFs derived by Brown et al. (2008). Webb et al. (2014) found that roughness configuration can have a significant effect on aeolian sediment transport. Surface heterogeneity moderates how much $u_*$is in excess of u_{*t} (Figure 4) and therefore both where erosion occurs within a landscape and the magnitude of the total flux from an eroding area. Sediment flux may vary by an order of magnitude for surfaces with the same λ but different roughness configurations (Figure 5). For very small λ, Q is found to increase with λ, as predicted by Yang and Shao (2005). R_t is found to be sensitive to roughness configuration, and this sensitivity needs to be accounted for in practical applications. The challenges identified by Webb et al. (2014) for implementing the Raupach et al. (1993) scheme for heterogeneous surfaces draw attention to alternative approaches to conceptualising the drag partition that explicitly represent the effect of heterogeneous roughness distributions on wind erosion.

[Insert Figure 4 here]

Figure 4: Histograms illustrating the effect of the 'random' and 'street' roughness configurations on wind shear velocity (u_*) calculated from measured surface shear stress (τ_s) distributions at a roughness density $\lambda = 0.1$ and four free stream wind velocities (U_f). Inset graphs show the proportion of τ_s greater than a threshold shear velocity $u_{*t} = 0.25$ m s^{-1} for the random (Ra) and street (Str) configurations. These proportions are indicative of the relative sediment fluxes produced for the two roughness configurations.

[Insert Figure 5 here]

Figure 5: Graphs showing roughness configuration effects on horizontal sediment mass flux, Q, expressed as the ratio of Q for the 'clumped', 'random' and 'street' configurations relative to Q for the 'staggered' configurations at a range of λ and free-stream wind velocities, U_f.

3: Random Momentum Sinks: from Vegetation to Saltation

3.1 Owen Effect

During saltation, sand grains interact with the airflow and transfer momentum to the surface. The particle momentum flux leads to an increase in roughness length of the aeolian surface similar to the roughness increase induced by waves on the ocean surface (Charnock, 1955) or by the waving canopy of a vegetated surface. This is known as the Owen effect in the aeolian community.

Although the Owen effect was known (Bagnold, 1941), its explanation lacked a solid theoretical underpinning until the work of Raupach (1991). Having worked years on flow over complex terrains, MR^2 was naturally very familiar with the studies on vegetation as a momentum sink and immediately recognized that saltating particles behave like stochastic mobile momentum sinks in the saltation layer. For the flow in the saltation layer, saltation reduces the vertical gradient of the flow velocity, and for the flow outside the saltation layer, it increases the capacity of the surface in absorbing momentum thereby increasing z_0.

By using earlier available observations, Owen (1964) found that the saltation roughness length, z_{0s}, can be expressed as:

$$z_{0s} = A\frac{u_*^2}{2g} \tag{14}$$

with A being approximately 0.02, which is identical to the Charnock (1955) roughness length scheme for 'wavy' surfaces. Equation (14) is empirical and has two limitations: (a) z_{0s} does not naturally recover z_0 in the case of no saltation; and (b) the observations of Rasmussen et al. (1985) and Gillette et al. (1998) have shown that z_{0s} in the natural environment is much larger than the equation predicts. Raupach (1991) developed an analytical expression for z_{0s} by analyzing four inter-related quantities, namely, the mean wind speed, particle-borne momentum flux, air-borne momentum flux and saltation roughness length. Again, to simplify the analysis MR^2 made several assumptions in Raupach (1991):

- The total momentum flux is constant in the saltation layer and is composed of a particle-borne momentum flux, τ_p, and an air-borne momentum flux, τ_a, i.e., $\tau = \tau_a(z) + \tau_p(z)$
- τ_p decreases while τ_a increases monotonically with height, and it is required that
  $\tau_p(z) \to 0 \quad \text{for} \quad z \to \infty$
  $\tau_a(z) \to \rho u_*^2 \quad \text{for} \quad z \to \infty$
- The characteristic height of τ_p profile, H_s, is on the order of the particle-jump height, such that
  $H_s = b_r \dfrac{u_*^2}{2g}$
  with b_r being a coefficient
- Owen's self-limiting hypothesis for equilibrium saltation applies, i.e., $\tau_a(0) \to \rho u_{*t}^2$

One functional form for $\tau_a(z)$, which satisfies these constraints is:

$$\left(\frac{\tau_a}{\rho u_*^2}\right)^{1/2} = 1 - (1-r)\exp\left(-\frac{z}{H_s}\right) \tag{15}$$

with:

$$r = \begin{cases} u_{*t}/u_* & u_* \geq u_{*t} \quad \text{saltation case} \\ 1 & u_* < u_{*t} \quad \text{no saltation case} \end{cases}$$

The wind profile in the saltation layer should obey:

$$\frac{\tau_a}{\rho} = K_m \frac{dU_h}{dz} \tag{16}$$

with the eddy diffusivity, K_m, defined as:

$$K_m = \kappa z \sqrt{\frac{\tau_a}{\rho}}$$

Further manipulation gives the wind profile within and above the saltation layer. From the wind profile above the saltation layer, MR^2 obtained the Raupach (1991) scheme for saltation roughness length:

$$z_{0s} = \left(A \frac{u_*^2}{2g}\right)^{(1-r)} z_0^{\,r} \tag{17}$$

Raupach (1991) suggested that a likely value for A, based on theoretical considerations, is 0.22.

Equation (17) shows that z_{0s} is a weighted geometric mean of z_0, the roughness length of the underlying surface and $Au_*^2/2g$. The latter is proportional to the characteristic height of the saltation layer, H_s. In Eq. (17), z_{0s} has two limiting values: when 1) there is no saltation, $r = 1$ and $z_{0s} = z_0$, and when 2) there is strong saltation, $r \to 0$ and $z_{0s} = A\ H_s$.

At the time when Raupach (1991) was published, little observational data were available to test the scheme. The experiments by Gillette et al. (1997; 1998) at Owens Lake, California provided one of the first tests of the Raupach (1991) scheme. A comparison of the observed and modelled z_{0s} is given in Figure 6, which shows that the measurements of z_{0s} can be well-described by Eq. (17) using $A = 0.38$, a value remarkably close to the predicted value of 0.22. This example is illustrative of many of Raupach's contributions that are built and sustained by a solid theoretical basis but easy to use for the interpretation of observations or the parameterization.

[Insert Figure 6 here]

Figure 6: Modelled saltation roughness length z_{0s} using Eq. (17) versus field measurements of Gillette et al. (1998).

Equation (15) is the key assumption of the Raupach (1991) model. This assumption is not concerned with how particles move in the saltation layer and has neglected the possible dependence of τ_p on the size of saltation particles. The fact that A is a function of saltation particle size is the likely reason Raupach's first approximation of 0.22 was less than the A value of 0.38 observed by Gillette et al. (1998).

In fact, an infinite number of profiles of τ_a satisfy the requirements proposed by MR^2, but we do not really know how τ_a changes with height in the saltation layer, in that there are very few available direct measurements of τ_a. The measurements of Li and McKenna Neumann (2012) show that shear stress profile in the saltation layer is strongly convex decreasing as the surface of the mobile bed is approached. Another unsolved issue is that Raupach (1991) did not account for the effect of turbulence on saltation trajectories. We can, for example, speculate that increased turbulence should increase the randomness of particle trajectories, and thereby intensify the Owen effect and increase the saltation roughness length. Raupach (1991) may have assumed that the randomness of saltation only causes a secondary effect in particle momentum transfer but this assumption needs testing.

It is not difficult to see that the issues dealt with in Raupach (1991, 1992) and Raupach et al. (1993) are related. In essence, due to the pressure drag on surface roughness elements, roughness length becomes a function of roughness configuration (in the simplest case, frontal area index, λ). In the case of vegetation, roughness elements are plants, and in the case of saltation, roughness elements are randomly moving particles.

3.2 Roughness length, issue of scale, and the albedo analogy

As an extension of Raupach (1992), Raupach (1994) proposed a scheme for computing roughness length for climate models. With the simplification of Raupach (1992), Eq. (12) becomes:

$$\kappa^2 \ln^{-2}\left(\frac{z-d}{z_0}\right) = (1+\beta\lambda)C_s \exp\left(-c\frac{\lambda U_h}{u_*}\right) \tag{18}$$

Equation (18) is the starting point of the Raupach (1994) scheme, which gained great popularity in the remote sensing community (Schaudt and Dickinson, 2000; Nakai et al., 2008; Tian et al., 2011). Raupach's work inspired Adrian Chappell to make the analogy between aerodynamic sheltering and shadow to retrieve aerodynamic properties over areas to provide a measure that scales linearly from the ground to remote sensing platforms (airborne or satellite) thereby tackling the four challenges of Raupach and Lu (2004) described in Section 2.4.

As discussed in Section 2, the momentum extracted by roughtons is controlled primarily by λ, i.e., a projection of roughness density in the direction of wind. When the projection is represented as a zenith angle α, $\tan(\alpha)$ can be seen as a multiplication factor which when restricted to 45° has a value of 1 and results in the projection of the entire frontal area of the roughness element $\lambda_p = \lambda \tan(\alpha)$. To simplify the problem, Raupach (1992) introduced the ideas of sheltering area and sheltering volume that vary with u_*/U_h as shown in Fig. 2 and Equation (3).

However, it is unlikely that the two dimensional measure λ can adequately characterize the three dimensional nature of aerodynamic roughness (Figure 7). If geometry projected to the surface is made a function of λ_p with $\alpha = \tan^{-1}(u_*/U_h)$ it should represent the shear stress (u_*/U_h) and the aerodynamic roughness length (z_0/h). Consequently, Raupach's effective shelter area is changed from a wedge. The new plan-form projection of shadow therefore assumes that u_*/U_h and z_0/h of wind from a particular direction is dependent on the zenith and azimuth illumination angles. This single scattering albedo was estimated to avoid any dependency on illumination and viewing conditions and to approximate the data available from remote sensing.

[Insert Figure 7 here]

Figure 7: Roughtons protect a portion of the substrate surface (a) that may include all or part of other roughness elements in a heterogeneous surface and following MR^2 may be considered dependent on u_*/U_h . A change in wind direction (b) redefines the sheltering effect demonstrating the anisotropic nature of the sheltering.

Chappell et al. (2010) then showed that the single scattering albedo is related to the z_0/h from wind velocity profiles of a range of surface roughness conditions in a wind tunnel (Dong et al., 2002). The albedo of the wind tunnel surface roughness was obtained retrospectively by reconstructing a digital elevation model (DEM) of the surface and then ray-casting.

Recent work, with several of the contributors to this paper, has further developed this approach using Marshall's (1971) seminal data. It is now evident that there is a relationship between albedo and many of the essential aerodynamic properties for wind erosion and dust emission modelling (e.g., u_*/U_h). Thus, it appears that this reduced complexity approach inspired by MR^2, enables consistent, repeatable and scalable areal estimates of aerodynamic properties. For example, the global MODIS MCD43A3 albedo product can be used to provide estimates of aerodynamic properties every 500 m and every 8 days between 2000 and present. Figure 8 shows u_*/U_h and lateral cover (L) for Australia on January 1, 2013.

[Insert Figure 8 here]

Figure 8: Examples of aerodynamic properties (a) u_*/U_h and (b) lateral cover estimated from the MODIS MCD43A3 albedo product (500 m resolution) for Australia 1 Jan 2013.

There appears to be considerable potential for this approach to provide consistent and repeatable estimates of aerodynamic properties and aeolian transport potential. This potential stems from the analogy that albedo and shadow mimic the sheltering effect of roughtons and albedo can be retrieved from ground-based (promixal) or remote sensing for large areas, making it a valuable proxy to aerodynamic roughness length. This analogy is probably well justified if roughness elements are sufficiently small compared to boundary-layer depth to exert significant influence on the flow structure, as assumed in Raupach (1992). However, because momentum transfer (governed by the Navier-Stokes equation) and radiation transfer (governed by the radiation transfer equation) have fundamentally different dynamic behavior (in particular non-linear interactions), it remains to be demonstrated whether such an analogy exists on a wider spectrum of scales. Nevertheless, it is a prime example of Raupach's inspiration to strive for a practical compromise between parsimony and fidelity in the representation of wind erosion and dust emission modelling of Raupach and Lu (2004) described above in Section 2.4.

4: Dust Emission and Saltation Bombardment

It is already evident in Gillette (1981) that the mechanisms for the entrainment of sand and dust particles differ, because the relative importance of the forces acting on them changes with particle size. The lift-off of sand particles is determined primarily by the balance between the aerodynamic and gravity forces. For smaller particles, the dominance of the gravity force diminishes and the inter-particle cohesion becomes important. It is now known that the gravity force is proportional to d^3, the aerodynamic force is proportional to d^2, and although large uncertainties exist in the estimates of cohesive forces, the total cohesive force is proportional to d. For particles with $d < 20$ μm, the cohesive force begins to dominate and hence particles cannot be easily lifted from the surface by aerodynamic forces. Dust particles under natural conditions exist as dust coatings attached to sand grains in sandy soils or as aggregates in clay soils. During weak wind-erosion events, sand particles coated with dust and clay aggregates behave as individuals and the adhering particles may not be released, while during strong wind-erosion events, dust coatings and soil aggregates may disintegrate, resulting in stronger dust emission. Three dust-emission mechanisms are recognized (Figure 9):

- *Aerodynamic Lift*: Dust particles can be lifted from the surface directly by aerodynamic forces. As the importance of gravity and aerodynamic forces diminishes for smaller particles and the inter-particle cohesion becomes more important, dust emission arising from direct aerodynamic lift is probably small in general;
- *Saltation Bomba*rdment: Dust emission is generated by saltation. As saltating particles (sand grains or aggregates) strike the surface, they cause localized impacts that are strong enough to overcome the binding forces acting upon soil dust particles, leading to dust emission. This mechanism is also known as sand blasting or aeolian abrasion (Alfaro et al., 1997; Bullard and White, 2005).
- *Disaggregation*: If saltating grains have dust coatings or if soil aggregates are transported in saltation, the energy exerted on the aggregates during impact can lead to their disaggregation and the release of dust particles. This process is called aggregate disintegration or auto/self-abrasion (e.g., Gillette, 1974; Chappell et al., 2008).

We can formally express the dust-emission rate arising from these three mechanisms as:

$$F = F_a + F_b + F_c \quad (19)$$

where F_a denotes aerodynamic lift, F_b saltation bombardment, and F_c aggregate disintegration.

[Insert Figure 9 here]

Figure 9: Mechanisms for dust emission. (I) Dust emission by (a) aerodynamic lift, (b) saltation bombardment and (c) aggregate disintegration. Traditionally, these processes are considered to be driven by mean wind shear, but large eddies can also cause intermittent sand drift and dust emission. (II) Illustration of particle lifting caused by the momentum intermittently transported to the surface by turbulent eddies. Saltation may be involved but does not need to be. (I) modified from Shao (2008) and (II) modified from Klose and Shao (2013).

In 1991, Yaping Shao began a postdoctoral position at the Pye Lab under the supervision of MR^2 to conduct wind-erosion related research. For conducting the experiments, the portable wind tunnel of John Leys was set up in front of the Pye Lab. MR^2 originally planned to test some of the theories that were then developing (e.g., Anderson and Haff, 1991) on saltation feedback (Shao and Raupach, 1992). One day, the then Australian Federal Minister for Environment (Hon. Mr. Ross Free) came to visit the Pye Lab. Raupach et al. were to demonstrate the problem of wind erosion. Soil was placed on the tunnel floor and the wind tunnel was started but no serious dust emission occurred and the Minister was not impressed. The idea of saltation bombardment came to MR^2 who then placed sand in front of the dust and produced for the Minister a mini dust storm using the wind tunnel. This story was the origin of the ideas tested in Shao et al. (1993). In that experiment they prepared two beds of material in the wind tunnel: an upstream sand bed which produced a supply of saltating grains, followed immediately by a dust bed that was subject to saltation bombardment. They used combinations of four sand-particle sizes (150, 250, 300 and 600 μm) and three dust-particle sizes (3, 11 and 19 μm). Shao et al. (1993) reported that there was little dust emission even at the maximum flow speed that the tunnel generated (~20 m s^{-1}) if no saltation particles were introduced, while strong dust emission occurred if sand particles were propelled over the dust surface. Soon thereafter, a similar wind-tunnel experiment was carried out by Alfaro et al. (1997) at the Laboratoire Interuniversitaire des Systèmes Atmosphériques (LISA). Their wind-tunnel experiments not only demonstrated the importance of saltation bombardment on dust emission, but also the emission of more small particles in the case of stronger saltation. What was learned from these experiments is that dust emission is in general proportional to streamwise saltation flux, i.e., $F \propto Q$.

It was soon recognized that the $F \propto Q$ relationship must be soil type dependent. Based on this understanding and using the data of Gillette (1979), Marticorena and Bergametti (1995) proposed the semi-empirical relationship:

$$F = 100 \exp(0.308 \cdot \eta + 13.82) Q \quad (20)$$

where η is percentage of clay content in the parent soil, and F and Q must be, respectively, in μg m^{-2} s^{-1} and μg m^{-1} s^{-1}. Many attempts have been made to develop physically-based dust emission schemes (e.g., Shao et al. 1993, 1996) while it is well-recognized that such efforts are complicated by the fact that the ratio F/Q must also depend on saltation particle size (how much kinetic energy is available) and on soil surface conditions (soft or hard surface, and the strength of cohesive binding forces e.g., Lu and Shao, 1999; Chappell et al., 2008; Kok et al., 2014a).

Attempts soon followed to develop schemes capable of predicting size-resolved dust emission, also called spectral dust emission schemes (e.g., Alfaro and Gomez, 2001; Shao et al. 2011).

The major challenge here is understanding the binding characteristics of dust particles and how they vary in space and time and change with particle size. There is so far insufficient understanding of dust-particle binding strength, but we know from Zimon (1982) that this strength has a stochastic component.

One possible way of overcoming this difficulty is to make use of the observed parent-soil particle size distribution (PSD). It is known from laboratory analysis that minimally dispersed and fully dispersed PSDs $p_m(d)$ and $p_f(d)$ are profoundly different. It is plausible to assume that dust aerosol PSD, $p_s(d)$, is confined by two limits:

$$p_s(d) = \gamma p_m(d) + (1-\gamma) p_f(d) \tag{21}$$

where γ is the weight for $p_m(d)$ and $(1-\gamma)$ for $p_f(d)$. Shao (2004) suggested that the emission of dust particles of size d_i arising from the saltation of d_s is given by:

$$\hat{F}_{di}(d_s) = c_y \left[(1-\gamma) + \gamma\sigma_d\right](\eta_{fi}\sigma_m + \eta_{ci})\frac{Qg}{u_*^2} \tag{22}$$

The integration over a range of sand-sized particles gives F_{di}, and the sum of F_{di} over all dust particle size bins gives the total dust emission, F. The process of saltation bombardment is embedded in the parameter $\sigma_m = m_\Omega / m_s$, the ratio between the mass ejected by bombardment, m_Ω, and the mass of the impacting particle, m_s, and in the parameter $\sigma_d = p_m(d_i)/p_f(d_i)$.

Due to the lack of observational data, spectral dust emission schemes were not sufficiently tested earlier. More recently, size-resolved dust fluxes have been estimated from field measurements of dust concentration (Sow et al., 2009). Ishizuka et al. (2014) conducted in Australia a sophisticated field experiment, in which dust emission for several particle sizes was determined. Shao et al. (2011) were able to use these data to calibrate the Shao (2004) scheme.

Over time a considerable amount of air-borne dust PSD data have been collected around the world. While differences in these PSDs exist, when they are plotted in one graph the differences do not seem to be overwhelming (Figure 10). This leads to the suggestion, that airborne dust PSD may be universal. There are rational arguments for the approach adopted by Shao (2004), i.e., Eq. (21). However, in hindsight the laboratory measurements of minimally dispersed and fully dispersed PSD do not provide appropriate constraints to $p_s(d)$, because the present-day available $p_m(d)$ is already close to the $p_s(d)$ at maximum saltation intensity, while $p_f(d)$ is simply not achievable through mechanical abrasion.

Although physics based dust emission schemes that require the properties of soil as input for determining size-resolved dust emission is justifiable, this increases the practical difficulty of implementation in large-scale models, such as global climate models (GCMs). Consequently, some climate models use ad hoc or empirical assumptions to describe the size distribution of emitted dust aerosols (e.g., Zender et al., 2003; Mahowald et al., 2006a; Yue et al., 2010).

Previous research showed that stressed dry soil aggregates fail as brittle materials (Lee and Ingles, 1968; Braunack et al., 1979; Perfect and Kay, 1995; Zobeck et al., 1999). Consequently, Kok (2011b) considered that most dust emission results originated from the fragmentation of aggregates due to saltation bombardment or self-abrasion. Since aggregate fragmentation is a form of brittle fragmentation, the size distribution produced by this process should be scale-invariant for a limited range (Astrom, 2006). The lower limit of this range is set by the size of the aggregate constituent particles, whereas the upper limit is set by the size of the aggregate. Kok (2011b) proposed that the size distribution of dust aerosols can be described by

$$\frac{\mathrm{d}V_{\mathrm{d}}}{\mathrm{d}\ln d} = \frac{d}{c_{\mathrm{V}}}\left[1+\mathrm{erf}\left(\frac{\ln\left(d/\bar{d}_s\right)}{\sqrt{2}\ln\sigma_{\mathrm{s}}}\right)\right]\exp\left[-\left(\frac{d}{\gamma}\right)^3\right] \qquad (23)$$

where V_d is the normalized volume of dust aerosols with geometric diameter d, c_v is a normalization constant, σ_s and $\bar{d}_{\mathrm{s}}$ are the geometric standard deviation and median diameter by volume of the log-normal distribution of a typical arid soil size distribution in the 20 μm size range, and the parameter γ denotes the propagation distance of side branches of cracks created in the dust aggregate by a fragmenting impact. Based on measurements of arid soil size distributions (Dalmeida and Schutz, 1983; Goldstein et al., 2005), Kok (2011b) obtained σ_s = 3.0 and $\bar{d}_{\mathrm{s}}$ = 3.4 μm. Furthermore, least-square fitting to dust PSD measurements yielded γ = 12 ±1 μm, such that c_v = 12.64 μm.

Equation (23) is in good agreement with measurements (Figure 10) of the dust PSD at emission. Note that the newest measurements of Rosenberg et al. (2014) suggest a larger fraction of very fine particles than previous measurements, indicating that more measurements of the dust size distribution are needed. Notably, apart from the Rosenberg et al. (2014) study, the scatter from the different measurements is quite limited, implying that differences in the wind speed and soil size distribution produce only limited variability in the emitted dust size distribution (Reid et al., 2008; Kok, 2011a).

Kok et al. (2014b) developed a new dust emission scheme (referred hereafter as K14), the underpinnings of which remains saltation bombardment, now combined with the hypothesis that most dust emission is produced by aggregate fragmentation. K14 shows better agreement against a compilation of dust flux measurements than the previous schemes of Gillette and Passi (1988) and Marticorena and Bergametti (1995), both of which are widely used in climate models (Huneeus et al., 2011). Furthermore, the implementation of K14 into the Community Earth System Model produces an improved simulation of the dust cycle (Kok et al., 2014a). This improved agreement is at least partially due to accounting for two processes that were not included in previous parameterizations. First, K14 accounts for the increasing scaling of dust flux with wind speed that occurs as a soil becomes less erodible and only the most energetic saltators become capable of producing dust. Second, K14 accounts for the decrease in dust production per saltator impact that occurs as the soil becomes less erodible. This important effect was previously realized by Shao et al. (1993), and included in the physically-explicit dust emission schemes of Shao et al. (1996), Shao (2001), and Shao (2004), but it is not included in dust emission schemes used in climate models.

[Insert Figure 10 here]

Figure 10: Compilation of measurements of the volume size distribution of dust aerosols at emission (colored data), compared with the theoretical prediction from brittle fragmentation theory (dashed line). Measurements by Gillette and colleagues (Gillette et al., 1972; Gillette, 1974; Gillette et al., 1974) were taken in Nebraska and Texas and used optical microscopy, whereas measurements by Fratini et al. (2007), Sow et al. (2009), and Shao et al. (2011) used optical particle counters and were respectively taken in China, Niger, and Australia. All these measurements were made on the ground during wind erosion events. In contrast, the measurements of Rosenberg et al. (2014) were made from an airplane flying over the northwestern Sahara, and used high-frequency optical particle counters to obtain the size-resolved dust flux from eddy covariance. All measurements were normalized following the procedure described in Kok (2011b) and Mahowald et al. (2014).

The insight that saltator impact speed determines the energy available for dust entrainment is to date an underlying assumption of all dust emission schemes based on saltation bombardment, irrespective of whether the emission process is then described in terms of energy balance (Shao et al., 1993, 1996; Alfaro and Gomes, 2001), soil dust particle abundance (Marticorena and Bergametti, 1995), volume removal (Shao, 2001, 2004), or fragmentation (Kok, 2011; Kok et al., 2014a, b). The fragmentation process introduced by Kok (2011) gives a specification on the binding energy that scales with particle size, which is consistent with the understanding that inter-particle cohesive force scales with particle size. As we have rather poor understanding of the particle binding strength, the fragmentation assumption offers a reasonable approximation. Given the fact that most observed dust aerosol particle size distributions can be reasonably well represented (Figure 10), indicates the approximation is useful.

Despite the significant progress made in dust emission modelling during the recent decades, the existing dust schemes contain weaknesses that are still a focus of current research efforts. As Raupach and Lu (2004) already stated in 2004, these weaknesses "include difficulties in application at large spatial and temporal scales, because of input data availability, parameter measurability, and large-scale variability in microphysical parameters and soil properties".

In most dust emission schemes, u_* and u_{*t} are decisive for the calculation of saltation and dust emission flux. Both u_* and u_{*t} are spatio-temporally integrated quantities and do not describe sub-grid scale and sub-measurement scale variability. No emission is predicted if $u_* < u_{*t}$. However, measurements show that aeolian activities can occur intermittently even if $u_* < u_{*t}$ holds on average (Stout and Zobeck, 1997; Wiggs et al., 2004). Recent studies have focused on intermittent saltation and achieved progress in its numerical modelling. For example, Dupont et al. (2013, 2014) reproduced the development of aeolian streamers due to turbulent eddies by implementing a saltation model in a large-eddy simulation framework.

Aerodynamic dust entrainment has received little attention until recently. This has two reasons: (1) theoretical considerations on inter-particle cohesion suggest that cohesive forces are too strong for particles in the dust-size range to be directly entrained; and (2) dust entrainment without saltation as observed in wind tunnels is much smaller than with saltation. However, considering the stochastic behaviour of inter-particle cohesion due to the multiple influencing factors, such as particle shape, particle surface roughness, or composition, leads to a wide range of scatter even for particles of similar size (Zimon, 1982; Shao, 2008).

A few studies show that dust emission can occur in the absence of saltation, but with much smaller magnitude (e.g., Shao et al., 1993; Loosmore and Hunt, 2000). However, these studies had been set up to study dust entrainment at different mean wind speeds and were not designed to investigate the influence of atmospheric turbulence. Turbulence can have coherent structures induced by buoyancy under unstable atmospheric conditions or by roughness elements as described for vegetation canopies by Raupach et al. (1996). This leads to surface momentum fluxes much larger than the mean wind speed suggests. Convective turbulence is most pronounced in the absence of strong mean winds, i.e., below the saltation threshold. Figure 11 (Klose and Shao, 2013) shows an example of dust emission generated by convective turbulence modelled with large-eddy simulation. At locations A (micro-convergence lines), B (micro-bursts) and C (vortices), significant dust emission may occur. Due to the stochastic nature of cohesive and turbulent aerodynamic lifting forces, aerodynamic dust entrainment is possible (Klose and Shao, 2012, 2013). In extreme cases (e.g., dust devils), turbulent dust emission can reach the magnitude typical for dust emission induced by saltation bombardment, but in most cases it is typically one to two orders of magnitude smaller. As turbulent dust emission occurs frequently, it may contribute significantly to the global dust cycle (Klose et al., 2014; Li et al., 2014).

[Insert Figure 11 here]

Figure 11: Turbulent wind speed (vectors, in m s^{-1}) and instantaneous turbulent momentum flux (black contour lines at 1 N m^{-2}) at 10 m height together with turbulent dust emission (shaded, in μg m^{-2} s^{-1}). Updated from Klose and Shao (2013) by the inclusion of the dust emission scheme of Klose et al. (2014).

5: Threshold friction velocity

5.1 Threshold as control parameter

Shields (1936) studied the threshold friction velocity, u_{*t}, for a spherical particle placed on a bare flat surface, by considering the balance between the gravity force and hydrodynamic drag. He introduced the dimensionless threshold shear stress

$$A = \frac{\tau_{*t}}{(\rho_p - \rho_f) g d} \quad (24)$$

and suggested that A is a function of only the particle Reynolds number, Re_{*t} ($= u_{*t}\, d/\nu$, where ν is kinematic viscosity). In Eq. (24), ρ_p and ρ_f are respectively the particle and fluid density. Bagnold (1941) derived a similar expression for wind-erosion threshold friction velocity and found that for large Re_{*t}, A is nearly constant and $u_{*t} \propto \sqrt{d}$. Wind-tunnel experiments of windblown sand simulating the atmospheric conditions on Mars and Venus with different kinematic viscosities and/or air densities suggested that Bagnold's expression works well for particles with $d > 100$ μm , but largely under-estimates u_{*t} for $d < 100$ μm (Greeley and Iversen, 1985). Iversen and White (1982) pointed out that the rapid increase of u_{*t} with decreasing particle size is caused by inter-particle cohesion. This led to a revised expression of the dimensionless threshold shear stress A that depends on the inter-particle force, I_p, in addition to Re_{*t}. The Iversen-White scheme is however rather complex. Shao and Lu (2000) advanced this approach by explicitly considering I_p as inversely proportional to d. This led to a much simpler expression of u_{*t} with the dimensionless shear stress A remaining as a function of Re_{*t} only. This new expression has been widely used for estimate of threshold velocity in air and as a reference for other planetary conditions (Burr et al., 2015).

MR^2 and Hua Lu collaborated on several research topics, one of which was soil erosion by wind and water. They explored the question why experimentally derived values of A are consistently higher than the theoretical estimates, and identified several real-world factors that may have major effects on A. These include soil cohesion that can be influenced by temperature and humidity, soil moisture, surface crusting and sheltering effect by roughness elements (McKenna Neuman, 2004). They also considered to what extent temperature-dependent changes in air density and viscosity could play a role in explaining the discrepancies between the observed and theoretical threshold velocities. Such discussion and other topics that related to more general wind erosion modelling led to the review of Raupach and Lu (2004) on the representation of land-surface processes in aeolian transport.

Along this line, MR^2 and Lu worked in greater detail to solve the observed puzzle of the Shields' A versus Re_{*t} diagram. When the data obtained from various experiments in air and in water are plotted on the typical Shields' diagram, they do not collapse to a single curve (Figure 12). What is then the reason for the departure between the data taken in air and water? Lu et al. (2005) proposed a more general expression of A, by incorporating the characteristics of near surface turbulence characterised by the flow Reynolds number $Re_\tau = u_*\delta/\nu$, where δ is the depth of the boundary-layer (Marusic and Kunkel, 2003). They showed that near surface flow velocity increases with Re_τ, and the typical values of Re_τ for air are several orders of magnitude larger than those for water. The large Re_τ in air is associated with intense near-bed turbulence that is dominated by gust-like eddy motions with length scales determined by the characteristic length scale of the roughness (Raupach et al., 1991, 1996). These gusts cause the streamwise velocity to show significant departure from a normal velocity distribution (Morrison et al., 2004), with a strong positive skewness near the bed. Conversely, in water, the mean flow above the layer where the particle entrainment occurs is mostly laminar. This results in a close to normal velocity distribution and smaller length scale of the roughness, therefore smaller values of Re_{*t} and A. They also demonstrated that the upturn of A for small Re_{*t} can also be affected by the background flow conditions apart from inter-particle cohesion. As such, they showed that their generalised expression achieves a consistent agreement with data for particle uplift in both air and water flows. Based on their analysis, they suggested that caution is needed in applying previous analytical and semi-empirical models. Perhaps more importantly, they pointed out that incorporating statistical descriptions of the mean flow condition may lead to noticeable improvement of wind erosion models. Indeed, these insights of MR^2 and Lu provided the basis for current research based on statistical description, as shown in Klose and Shao (2012, 2013), and some of the aspects considered in Kok et al. (2014b).

[Insert Figure 12 here]

Figure 12: Dimensionless threshold shear stress A as a function of particle Reynolds number Re_{*t} based on data obtained in water flow (filled) and in air stream (unfilled). These two groups of observations depart both at the large Re_{*t} regime, where aerodynamics dominates and for small Re_{*t} values, where particle cohesion becomes important in determine A. From Lu et al. (2005).

6: The Carbon Link

Soil stores up to 80% of the organic carbon in the terrestrial biosphere and contains more than three times the soil organic carbon (SOC) in the atmosphere (Lal, 2003). The C pools are interconnected and thus a disturbance of the terrestrial C pool (e.g. by soil erosion) can introduce significant changes in the atmospheric C pool. The amount of carbon dioxide (CO_2) captured and converted to SOC annually via terrestrial net primary productivity (NPP) or released as CO_2 by soil microbial respiration (R) is about an order of magnitude greater than the annual increase in atmospheric CO_2 (Houghton et al., 1992). Soil therefore represents a substantial component in the global carbon cycle and small changes in the SOC stock may result in large changes of atmospheric CO_2 (Giorgi, 2006).

Wind-erosion generated dust emission/deposition and the associated SOC exchange between the atmosphere and soil constitutes an important part of the dust-cycle and carbon-cycle interactions, along with the dust-iron effect on the atmosphere and ocean CO_2 exchange (Shao et al., 2013). For more than two decades (early 1990s to 2015), MR^2 worked extensively on the global carbon budget and made a fundamental contribution to that research (Field and Raupach, 2012). MR^2 realized early the importance of wind-erosion driven soil nutrient and organic carbon transport, and pointed out that wind erosion removes preferentially the fine, nutrient- and SOC-rich top soil, reduces the soil water holding capacity and thereby causes land degradation (Raupach et al. 1994). Raupach et al. (1994) provided an assessment of soil nutrient loss, in terms of Nitrogen (N), Phosphorous (P) and Potassium (K), caused by the 1983 Melbourne dust storm. While time did not permit MR^2 to work directly on the SOC problem in relation to wind erosion, his initial work was continued by the Australian aeolian research community and in particular Butler, Chappell, Strong and Webb who established the foundation for relating continental estimates of wind erosion (CEMSYS; Shao, 2000) to SOC.

For example, Chappell et al. (2014) described how SOC dust emission is omitted from Australian national C accounting and is an underestimated source of CO_2. They developed a first approximation to SOC enrichment for the dust emission model CEMSYS and quantified SOC dust emission for Australia (5.8 Tg CO_2-e/y) and Australian agricultural soils (0.4 Tg CO_2-e/y). These amounts under-estimate CO_2 emissions by approximately 10% for the combined C pools in Australia (based on 2000 estimates), with approximately 5% derived from Australian rangelands and 3% of Australian agricultural soils using the Kyoto accounting method. Northern hemisphere countries with greater dust emission than Australia are also likely to have much larger SOC dust emission. Therefore, omission of SOC dust emission likely represents a considerable underestimate from those nation's C accounts. Chappell et al. (2014) suggested that the omission of SOC dust emission from C cycling and C accounting is a significant global source of uncertainty.

7: Summary

In this tribute, we reviewed Raupach's work on aeolian fluid dynamics and the impact of his work on the progress of aeolian research. This is only a small part of Raupach's extensive studies on environmental mechanics and climate change (e.g., Field and Raupach, 2012; Raupach et al., 2014). Specifically for aeolian research, MR^2 helped to consolidate the foundation of aeolian fluid dynamics and aeolian modelling, and to propel aeolian research to become a core theme in earth system studies.

Raupach's pioneering work is linked directly to a number of conceptual and modelling advancements made in recent years, while at the same time opening numerous avenues that allowed the aeolian research community to make numerous advances toward our understanding of aeolian processes. Avenues of inquiry opened by MR^2 include:

(1) *Aeolian Processes over Heterogeneous Surfaces*: Ever since the 1940s, we have focused on studying aeolian processes of relatively simple surfaces, often under the assumption of surface homogeneity and uniform saltation. Thanks to Raupach (1991, 1992) and Raupach et al. (1993), and numerous field and numerical experiments, the essence of the momentum exchange between the atmosphere and aeolian surface is now understood. As we followed Raupach (1992) and Raupach et al. (1993), we realized that the spatial and temporal variations of momentum fluxes profoundly affect aeolian transport, which is in more general terms the typical case of heterogeneous aeolian transport. While research on this topic is rapidly progressing, as demonstrated by Webb et al. (2014) and Dupont et al. (2014), much more needs to be done to establish a theoretical framework and to develop predictive tools.

(2) *Stochastic and Statistical Dust Modeling*: Existing wind-erosion models are mostly of deterministic nature. However, aeolian processes involve stochastic variables, such as inter-particle cohesion or turbulent surface shear stress, as indicated in Raupach and Lu (2004). New developments in dust-emission models of a statistical nature have been made recently by Klose et al. (2014) and may herald a new generation of wind-erosion models in the coming years.

(3) *Integration of Aeolian Models with Ecological Models*: The carbon cycle is of central importance to climate studies. MR^2 devoted more than 20 years of his academic life to research on the global carbon budget. We now know that understanding of the carbon

cycle cannot be completed without knowledge of the dust cycle. This is because dust plays a pivotal role in the atmosphere and ocean CO_2 exchange and aeolian processes are vital for SOC transport and fixation. Thus, aeolian research plays a central role in global Earth system studies. For this to be adequately represented in Earth system models, the dust cycle needs to be better represented (e.g., Kok et al., 2014), but also the coupling of aeolian and ecological processes is important. For steppe landscapes the coupling of wind-erosion models with ecological models is developing (e.g., Shinoda et al., 2011). We expect that this effort will accelerate in the future.

(4) *New Measurements:* MR^2 was famous for his theoretical work, but he was also an accomplished experimental researcher and organizer. He conducted and organized numerous wind-tunnel (e.g., Raupach and Legg, 1983) and field experiments (e.g., Leuning et al., 2004). The very first talk MR^2 gave on wind erosion was at the 1st Australian Workshop on Wind Erosion entitled "How to Measure Wind Erosion?". It was an introductory talk on the basic techniques for saltation measurements. We have moved on since that time, and much more cohesive and sophisticated measurements can be made today. Size-resolved sand transport and dust emission measurements were made early on in Australia (Nickling et al., 1999), in Niger (Sow et al., 2009) and again in Australia in the Japan – Australian Dust Experiment (Ishizuka et al., 2014). New instruments such as PI- SWERL® (Etyemezian et al., 2014) and micro wind tunnel (Strong et al., 2015) have been developed for field measurements with emphasis on characterizing spatial variability of dust emissions.

(5) *Large-eddy Aeolian Simulation (LEAS):* The basic concept of aeolian transport process as a feedback system involving the atmosphere, land surface, and soil particles emerged in the early 1990s (Anderson and Haff, 1991). Earlier versions of LEAS models were developed by Shao and Li (1999) and Doorschot and Lehning (2002) among others. In more recent years, highly sophisticated LEAS models have been developed, for example, by Klose and Shao (2013) and Dupont et al. (2014). With these models, some of the hypotheses of MR^2 can now be fully tested, and more importantly LEAS models serve as powerful tools for generating in depth understanding for improved aeolian process parameterizations (Li et al., 2014; Klose et al., 2014).

For many of us, MR^2 was not only a role model scholar, but also a great colleague and a friend. A long-time colleague of MR^2 describes that his "excellence in scientific research is not the only skill that enabled Mike to build such a brilliant career. He always had a warm and thoughtful way of collaborating with his colleagues. He showed respect and humility in interacting not only with them, but also with the policy world and the public. Mike's communications skills were legendary. He could distil the most complex ideas into crisp, understandable stories. His words were carefully chosen, and his spoken sentences often carried the grace and power of expertly crafted written prose. His touchstone, however, was always the science, and in that he was unfailingly rigorous and insightful" (Steffen, 2015).

MR^2 was a modest person, always keen to learn from others and at the same time, he was a natural teacher for younger researchers worldwide. He made a large effort to nurture younger Australian aeolian researchers. Harry Butler, Paul Findlater, John Leys, Hua Lu and Yaping Shao all benefited immensely from his deep knowledge and enthusiasm for science. Long after MR^2 had moved on from aeolian studies, and he was swimming in the much larger research pool of global carbon budgeting, he continued to demonstrate his generosity and nurturing attitude towards students, as for example, when he advised Craig Strong on the fluid dynamics of a micro wind tunnel. In 2014, Strong took up a lectureship at ANU and months later MR^2 also arrived to take on the role of Director at the Climate Change Institute. Discussion recommenced between them, but sadly MR^2 passed away before the publication of their work (Strong et al., 2015).

Our community mourns the loss of MR^2 as a big thinker and influential leader and as this review demonstrates, his work provided many foundations for the current advances and new directions of aeolian research. As we follow in many of his footsteps and explore uncharted territories, Mike will be missed.

References

Alfaro, S. C., Gaudichet, A., Gomes, L., Maille, M., 1997. Modeling the size distribution of a soil aerosol produced by sandblasting. J. Geophys. Res. 102, 11239-11249.

Alfaro, S. C., Gomes, L., 2001. Modeling mineral aerosol production by wind erosion: Emission intensities and aerosol size distributions in source areas. J. Geophys. Res. 106, 18075-18084.

Anderson, R. S., Haff, P. K., 1991. Wind modification and bed response during saltation of sand in air. Acta Mechanica, Suppl. 1, 21-51.

Arya, S. P. S., 1975. A drag partition theory for determining the large-scale roughness parameter and wind stress on Arctic pack ice. J. Geophys. Res. 80, 3447-3454.

Astrom, J. A., 2006. Statistical models of brittle fragmentation. Adv. Phys. 55, 247-278.

Bagnold, R. A., 1941. The Physics of Blown Sand and Desert Dunes, Methuen, London.

Braunack, M. V., Hewitt, J. S., Dexter, A. R., 1979. Brittle-fracture of soil aggregates and the compaction of aggregate beds. J. Soil Sci. 30, 653-667.

Brown, S., Nickling, W. G., Gillies, J. A., 2008. A wind tunnel examination of shear stress partitioning for an assortment of surface roughness distributions. J. Geophys. Res. 113, F02S06, doi: 10.1029/2007JF000790.

Bullard, J. E., White, K., 2005. Dust production and the release of iron oxides resulting from the aeolian abrasion of natural dune sands. Earth Surf. Process. Landforms 30, 95–106. doi: 10.1002/esp.1148.

Burr, D. M., Bridges, N. T., Marshall, J. R., Smith, J. K., White, B. R., Emery, J. P., 2015. Higher-than-predicted saltation threshold wind speeds on Titan. Nature 517, 60-63.

Chappell, A., Zobeck, T., Brunner, G., 2005. Induced soil surface change detected using on-nadir spectral reflectance to characterise soil erodibility. Earth Surf. Proc. Landforms 30 (4), 489-511, http://dx.doi.org/10.1002/esp.1185.

Chappell, A., Zobeck, T.M., Brunner, G., 2006. Using bi-directional soil spectral reflectance to model soil surface changes induced by rainfall and wind-tunnel abrasion. Rem. Sens. Environ. 102 (3-4), 328-343, http://dx.doi.org/10.1016/j.rse.2006.02.020.

Chappell, A., Strong, C., McTainsh, G., Leys, J., 2007. Detecting induced in situ erodibility of a dust-producing playa in Australia using a bi-directional soil spectral reflectance model. Rem. Sens. Environ. 106, 508-524, http://dx.doi.org/10.1016/j.rse.2006.09.009.

Chappell, A., Dong, Z., Van Pelt, S., Zobeck, T., 2010. Estimating aerodynamic resistance of rough surfaces using angular reflectance. Rem. Sens. Environ. 114 (7), 1462-1470, http://dx.doi.org/10.1016/j.rse.2010.01.025.

Chappell, A., Webb, N.P., Viscarra Rossel, R.A., Bui, E., 2014. Australian net (1950s-1990) soil organic carbon erosion: implications for CO_2 emission and land-atmosphere modelling. Biogeosciences 11, 5235-5244, doi: 10.5194/bg-11-5235-2014.

Chappell, A., Baldock, J., Sanderman, J., 2015. The global significance of omitting soil erosion from soil organic carbon cycling models. Nature Climate Change (invited re-submission April 2015).

Chappell, A., Warren, A., O'Donoghue A., Robinson A., Thomas, A. and Bristow, C., 2008. The implications for dust emission modeling of spatial and vertical variations in horizontal dust flux and particle size in the Bodélé Depression, Northern Chad, J. Geophys. Res.-Atmos. 113, D04214, http://dx.doi.org/10.1029/2007JD009032.

Charnock, H., 1955. Wind stress on a water surface. Q. J. Roy. Met. Soc. 81, 639-640.

Crawley, D., Nickling, W.G., 2003. Drag partition for regularly-arrayed rough surfaces. Boundary-Layer Meteorol. 107, 445-468.

Dalmeida, G. A., Schutz, L., 1983. Number, mass and volume distributions of mineral aerosol and soils of the sahara. J. Climate and Appl. Meteorol. 22, 233-243.

Dong, Z., Liu, X., Wang, X., 2002. Aerodynamic roughness of gravel surfaces. Geomorphology 43 (1–2), 17−31.

Doorschot, J. J. J., Lehning, M, 2002. Equilibrium saltation: Mass fluxes, aerodynamic entrainment, and dependence on grain properties. Boundary Layer Meteorol. 104 (1), 111 – 130.

Dupont, S., Bergametti, G., Marticorena, B., Simoëns, S., 2013. Modeling saltation intermittency. J. Geophys. Res. 118, 7109 – 7128, doi: 10.1002/jgrd.50528.

Dupont, S., Bergametti, G., Simoëns, S., 2014. Modeling aeolian erosion in presence of vegetation. J. Geophys. Res.-Earth Surface 119, 168 – 187, doi: 10.1002/2013JF002875.

Etyemezian, V. R., Gillies, J. A., Shinoda, M., Nikolich, G., King, J., Bardis, A. R., 2014. Accounting for surface roughness on measurements conducted with PI-SWERL: Evaluation of a subjective visual approach and a photogrammetric technique. Aeolian Research 13, 35-50.

Field, C., Raupach, M. R., 2012. The Global Carbon Cycle: Integrating Humans, Climate, and the Natural World (Scientific Committee on Problems of the Environment (SCOPE) Series). Kindle Edition, Island Press, pp. 568.

Fratini, G., Ciccioli, P., Febo, A., Forgione, A., Valentini, R., 2007. Size-segregated fluxes of mineral dust from a desert area of northern China by eddy covariance. Atmos. Chem. Phys. 7, 2839-2854.

Gillette, D.A., 1974. On the production of soil wind erosion having the potential for long range transport. J. Rech. Atmos. 8, 734-744.

Gillette, D. A., 1979. Environmental factors affecting dust emission by wind erosion. In Morales, C. (ed.), Saharan Dust, 71-94. John Wiley, New York.

Gillette, D. A., 1981. Production of dust that may be carried great distances. Spec. Pap. Geol. Soc. Am. 186, 11 – 26.

Gillette, D.A., 1999. A qualitative geophysical explanation for "hot spot" dust emitting source regions. Contributions to Atmos. Phys. 72 (1), 67-77.

Gillette, D.A., Blifford, I. H., Fenster, C. R., 1972. Measurements of aerosol size distributions and vertical fluxes of aerosols on land subject to wind erosion. J. Appl. Meteor. 11, 977-987.

Gillette, D.A., Blifford, I. H., Fryrear, D. W., 1974. Influence of wind velocity on size distributions of aerosols generated by wind erosion of soils. J. Geophys. Res. 79, 4068-4075.

Gillette, D. A., Fryrear, D. W., Xiao, J. B., Stockton, P., Ono, D., Helm P. J., Gill, T. E., Ley, T., 1997. Large-scale variability of wind erosion mass flux rates at Owens Lake 1. Vertical profiles of horizontal mass fluxes of wind-eroded particles with diameter greater than 50 µm. J. Geophys. Res. 102, 25977-25987.

Gillette, D.A., Herrick, J., Herbert, G. A., 2006. Wind characteristics of mesquite streets in the northern Chihuahuan Desert, New Mexico, USA. Environ. Fluid Mech. 6 (3), 241-275.

Gillette, D.A., Marticorena, B., Bergametti, G., 1998. Changes in aerodynamic roughness height by saltating grains: experimental assessment, test of theory, and operational parameterization. J. Geophys. Res. 103, 6203-6209.

Gillette, D.A., Passi, R., 1988. Modeling dust emission caused by wind erosion. J. Geophys. Res. 93, 14233-14242.

Gillette, D.A., Pitchford, A., 2004. Sand flux in the northern Chihuahuan Desert, New Mexico, USA and the influence of mesquite-dominated landscapes. J. Geophys. Res. 109 (F04003), doi: 10.1029/2003JF000031.

Gillette, D. A., Stockton, P. H., 1989. The effect of nonerodible particles on wind erosion at erodible surfaces. J. Geophys. Res. 94, 12885 – 12893.

Gillies, J.A., Green, H., McCarley-Holder, G., Grimm, S., Howard, C., Barbieri, N., Ono, D., Schade, T., 2015. Using solid element roughness to control sand movement: Keeler Dunes, Keeler, California. Aeolian Research, doi: 10.1016/j.aeolia2015.05.004.

Gillies, J.A., Lancaster, N., 2013. Large roughness element effects on sand transport, Oceano Dunes, California. Earth Surf. Proc. Landforms 38 (8), 785-792, doi: 10.1002/esp.3317.

Gillies, J.A., Lancaster, N., Nickling, W. G., Crawley, D. M., 2000. Field determination of drag forces and shear stress partitioning effects for a desert shrub (*Sarcobatus vermiculatus*, greasewood), J. Geophys. Res. 105 (D20), 24871-24880.

Gillies, J.A., Nickling, W.G., King, J., 2002. Drag coefficient and plant form-response to wind speed in three plant species: Burning Bush (*Euonymus alatus*), Colorado Blue Spruce (*Picea pungens glauca*.), and Fountain Grass (*Pennisetum setaceum*). J. Geophys. Res. 107 (D24), 4760, doi: 4710.1029/2001JD001259.

Gillies, J.A., Nickling, W.G., King, J., 2006. Aeolian sediment transport through large patches of roughness in the atmospheric inertial sublayer. J. Geophys. Res. - Earth Surface 111 (F02006). doi: 10.1029/2005JF000434.

Gillies, J.A., Nickling, W.G., King, J., 2007. Shear stress partitioning in large patches of roughness in the atmospheric inertial sublayer. Boundary-Layer Meteorol. 122 (2), 367-396, doi: 10.1007/s10546-006-9101-5

Giorgi, F. 2006. Climate change hot-spots, Geophys. Res. Lett. 33, L08707.

Goldstein, H., Reynolds, R., Reheis, M., Yount, J., Lamothe, P., Roberts, H., McGeehin, J., 2005. Particle-Size, $CaCO_3$, Chemical, Magnetic, and Age Data from Surficial Deposits in and around Canyonlands National Park, Utah, U.S. Geological Survey.

Greeley, R., Iversen, J. D., 1985. Wind as a Geological Process on Earth, Mars, Venus and Titan, Cambridge University Press, New York.

Houghton, J. T., Callander, B. A., Varney, S. K. (Eds.), Climate Change 1992. The Supplementary Report to the IPCC Scientific Assessment, Report of the Intergovernment Panel on Climate Change. Cambridge University Press, New York.

Huneeus, N., Schulz, M., Balkanski, Y., Griesfeller, J., Prospero, J., Kinne, S., Bauer, S., Boucher, O., Chin, M., Dentener, F., Diehl, T., Easter, R., Fillmore, D., Ghan, S., Ginoux, P., Grini, A., Horowitz, L., Koch, D., Krol, M. C., Landing, W., Liu, X., Mahowald, N., Miller, R., Morcrette, J. J., Myhre, G., Penner, J., Perlwitz, J., Stier, P., Takemura, T., Zender, C. S., 2011. Global dust model intercomparison in AeroCom phase I. Atmos. Chem. Phys. 11, 7781-7816.

Ishizuka, M., Mikami, M., Leys, J. F., Shao, Y., Yamada, Y., Heidenreich, S., 2014. Power law relation between size-resolved vertical dust flux and friction velocity measured in a fallow wheat field. Aeolian Research 12, 87–99, doi: 10.1016/j.aeolia.2013.11.002.

Iversen, J. D., White, B. R., 1982. Saltation threshold on Earth, Mars and Venus. Sedimentology 29, 111–119.

Iversen, J. D., Wang, W. P., Rasmussen, K. R., Mikkelsen, H. E,. Leach, R. N., 1991. Roughness element effect on local and universal saltation transport. Acta Mech. Suppl. 2, 65-75.

King, J., Nickling, W. G., Gillies, J. A., 2005. Representation of vegetation and other non-erodible elements in aeolian sediment transport models. J. Geophys. Res. - Earth Surface 110 (F4), F04015, doi: 04010.01029/02004JF000281.

King, J., Nickling, W. G., Gillies, J. A., 2006. Aeolian shear stress ratio measurements within mesquite-dominated landscapes of the Chihuahuan Desert, New Mexico, USA. Geomorphology 82 (3-4), 229-244, doi: 10.1016/j.geomorph.2006.05.004.

Klose, M., Shao, Y., 2012. Stochastic parameterization of dust emission and application to convective atmospheric conditions. Atmos. Chem. Phys., 12, 7309-7320, doi: 10.5194/acp-12-7309-2012

Klose, M., Shao, Y., 2013. Large-eddy simulation of turbulent dust emission. Aeolian Research 8, 49-58, doi: 10.1016/j.aeolia.2012.10.010.

Klose, M., Shao, Y., Li, X., Zhang, H., Ishizuka, M., Mikami, M. Leys, J.F., 2014. Further development of a parameterization for convective turbulent dust emission and evaluation based on field observations. J. Geophys. Res. Atmos., 119, 10,441–10, doi: 10.1002/2014JD021688.

Kok, J. F., 2011a. Does the size distribution of mineral dust aerosols depend on the wind speed at emission? Atmos. Chem. Phys. 11, 10149-10156.

Kok, J. F., 2011b. A scaling theory for the size distribution of emitted dust aerosols suggests climate models underestimate the size of the global dust cycle. Proc. Natl. Acad. Sci. U. S. A. 108, 1016-1021.

Kok, J. F., Albani, S., Mahowald, N. M., Ward, D. S. 2014a. An improved dust emission model - Part 2: Evaluation in the Community Earth System Model, with implications for the use of dust source functions. Atmos. Chem. Phys. 14, 13043-13061.

Kok, J. F., Mahowald, N. M., Fratini, G., Gillies, J. A., Ishizuka, M., Leys, J. F., Mikami, M., Park, M. S., Park, S. U., Van Pelt, R. S., Zobeck, T. M., 2014b. An improved dust emission model - Part 1: Model description and comparison against measurements. Atmos. Chem. Phys. 14, 13023-13041.

Lal, R., 2003. Soil erosion and the global carbon budget. Environ. Int. 29, 437–450.

Lancaster, N., Baas, A., 1998. Influence of vegetation cover on sand transport by wind: field studies at Owens Lake, California. Earth Surf. Proc. Landforms 23, 69—82.

Lee, I. K., Ingles, O. G., 1968. Soil mechanics selected topics. In: The Brittle Failure of Unsaturated Soils, Stabilized Soils, and Rocks, Lee, I. K. (ed.), Elsevier, New York.

Lettau, H., 1969. Note on aerodynamic roughness-parameter estimation on the basis of roughness-element distribution. J. Appl. Met. 8, 828-832.

Leuning, R., M. R. Raupach, P. A. Coppin, H. A. Cleugh, P. Isaac, O. T. Denmead, F. X. Dunin, S. Zegelin, J. Hacker, 2004. Spatial and temporal variations in fluxes of energy, water vapour and carbon dioxide during OASIS 1994 and 1995. Boundary-Layer Meteorol. 110 (1), doi: 10.1023/A:1026028217081.

Leys, J. F., Raupach, M. R., 1990. Aerodynamics of a portable wind erosion tunnel for measuring soil erodibility by wind. Aust. J. Soil Res. 28, 177 – 191.

Li, A., Shao, Y., 2003. Numerical simulation of drag partition over rough surfaces. Boundary-Layer Meteorol. 108, 317—342 doi: 10.1023/A:1024179025508.

Li, B. L., McKenna Neuman, C., 2012: Boundary-layer turbulence characteristics during aeolian saltation. Geophys. Res. Lett. 39, L11402, doi:10.1029/2012GL052234.

Li, J., Okin, G. S., Herrick, J. E., Belnap, J., Miller, M. E., Vest, K., Draut, A. E., 2013. Evaluation of a new model of aeolian transport in the presence of vegetation. J. Geophys. Res. - Earth Surface 118, 288-306.

Li, X. L., Klose, M., Shao, Y., Zhang, H. S., 2014. Convective turbulent dust emission (CTDE) observed over Horqin Sandy Land area and validation of a CTDE scheme. J. Geophys. Res. Atmos. 119, 9980–9992, doi: 10.1002/2014JD021572.

Loosmore, G. A., Hunt, J. R., 2000. Below-threshold, non-abraded dust resuspension. J. Geophys. Res. 105, 20663-20671.

Lu, H., Shao, Y., 1999. A new model for dust emission by saltation bombardment. J. Geophys. Res. 104, 16827-16842.

Lu, H., Raupach, M. R., Richards, K., 2005. Entrainment of sedimentary particles by wind and water: similarities, differences and a general approach. J. Geophys. Res. 110, D24114, doi: 10.1029/2005JD006418.

Lyles, L., Allison, B. E., 1976. Wind erosion: the protective role of simulated standing stubble. Trans. Am. Soc. Agric. Engrs. 19, 61 – 64.

Mahowald, N., Albani, S., Kok, J. F., Engelstaeder, S., Scanza, R., Ward, D. S., Flanner, M. G., 2014. The size distribution of desert dust aerosols and its impact on the Earth system. Aeolian Research 15, 53-71.

Mahowald, N. M., Muhs, D. R., Levis, S., Rasch, P. J., Yoshioka, M., Zender, C. S., Luo, C., 2006a. Change in atmospheric mineral aerosols in response to climate: Last glacial period, preindustrial, modern, and doubled carbon dioxide climates. J. Geophys. Res. 111, D10202.

Mahowald, N. M., Yoshioka, M., Collins, W. D., Conley, A. J., Fillmore, D. W., and Coleman, D. B., 2006b. Climate response and radiative forcing from mineral aerosols during the last glacial maximum, pre-industrial, current and doubled-carbon dioxide climates, Geophysical Research Letters 33, L20705.

Marsh, B. and D. Carter, 1983. Wind erosion. Western Australian J. Agriculture 24 (2), 54-57.

Marshall, J. K., 1971: Drag measurements in roughness arrays of varying density and distribution, Agric. Meteorol. 8, 269– 292.

Marticorena, B., Bergametti, G., 1995: Modeling the atmospheric dust cycle: 1. Design of a soil derived dust production scheme, J. Geophys. Res. 100, 16,415– 16,430.

Marusic, I., Kunkel, G. J., 2003. Streamwise turbulence intensity formulation for flat-plate boundary layers. Phys. Fluids 15 (8), 2461–2464.

McKenna Neuman, C., 2004. Effects of temperature and humidity upon the transport of sedimentary particles by wind. Sedimentology 51, 1–18.

McTainsh, G.H., Leys, J.F. (1993). Wind Erosion. In: McTainsh, G.H., Boughton, W.C. (eds.), Land Degradation Processes in Australia. Longman-Cheshire, Melbourne, pp. 188-233.

Morrison, J. F., McKeon, B. J., Jiang, W., Smits, A. J., 2004. Scaling of the streamwise velocity component in turbulent pipe flow. J. Fluid Mech. 508, 99–131.

Musick, H. B., Gillette, D. A., 1990. Field evaluation of relationships between a vegetation structural parameter and sheltering against wind erosion. Land Degrad. Rehab. 2, 87-94.

Nabat, P., Solmon, F., Mallet, M., Kok, J. F., and Somot, S., 2012. Dust emission size distribution impact on aerosol budget and radiative forcing over the Mediterranean region: a regional climate model approach. Atmos. Chem. Phys. 12, 10545-10567.

Nakai, T., Sumida, A., Daikoku, K., Matsumono, K.. van der Molen, M., Kodama, Y., Kononov, V., Maximov, T. C., Dolman, A. J., Yabuki, H., Hara T., Ohta, T., 2008: Parameterization of aerodynamic roughness over boreal, cool- and warm-temperate forests. Agricul. Forest Meteorol. 148, 1916 – 1925.

Nickling, W.G., McTainsh, G.H., Leys, J.F., 1999. Dust emissions from the Channel Country of western Queensland, Australia. Zeitschrift für Geomorphologie N.F. 116, 1-17.

Nield, J. M., King, J., Wiggs, G.F.S., Leyland, J., Bryant, R. G., Chiverrell, R. C., Darby, S. E., Eckardt, F. D., Thomas, D. S. G., Vircavs L. H., Washington, R., 2013. Estimating aerodynamic roughness over complex surface terrain. J. Geophys. Res. - Atmospheres 118, 12948-12961, doi: 10.1002/2013JD020632.

Okin, G., 2008. Article: A new model of wind erosion in the presence of vegetation. J. Geophys. Res. – Atmospheres 113, doi: 10.1029/2007JF000758.

Owen, R. P., 1964. Saltation of uniform grains in air. J. Fluid Mech. 29, 407– 432.

Perfect, E., Kay, B. D., 1995. Brittle-fracture of fractal cubic aggregates. Soil Sci. Soc. Am. J. 59, 969-974.

Rasmussen, K. R., Sorensen, M., Willetts, B. B., 1985. Measurements of saltation and wind strength on beaches. In Barndorff-Nielsen, O. E., Möller, J. T., Rasmussen, K. R., Willets B. B. (eds.), Proceedings of the International Workshop on the Physics of Blown Sand, pp. 301—325.

Raupach, M. R., Legg, B. L., 1983. Turbulent dispersion from an elevated line source: Measurements of wind-concentration moments and budgets. J. Fluid Mech. 136, 111-137.

Raupach, M. R., 1991. Saltation layers, vegetation canopies and roughness lengths, Acta Mech. 1, Suppl., 83–96.

Raupach, M. R., R. A. Antonia, and S. Rajagopalan, 1991. Rough-wall turbulent boundary layers. Appl. Mech. Rev. 44, 1–25.

Raupach, M. R., 1992. Drag and drag partition on rough surfaces. Boundary Layer Meteorol. 60, 375– 395.

Raupach, M. R., 1994. Simplified expressions for vegetation roughness length and zero-plane displacement as functions of canopy height and area index. Boundary-Layer Meteorol. 71, 211 – 216.

Raupach, M. R., Gillette, D. A., Leys, J. F., 1993. The effect of roughness elements on wind erosion threshold. J. Geophys. Res. 98, 3023–3029.

Raupach M.R., McTainsh, G. H., Leys, J. F., 1994. Estimates of dust mass in recent major dust storms. Australian J. Soil and Water Conserv. 7 (3), 20-24.

Raupach, M.R., Finnigan, J.J., Brunet, Y., 1996. Coherent eddies and turbulence in vegetation canopies: the mixing layer analogy. Boundary-Layer Meteorol. 78, 351-382.

Raupach, M. R., Lu, H., 2004. Representation of land-surface processes in aeolian transport models. Environ. Modelling & Software 19, 93–112.

Raupach, M. R., Davis, S. J., Peters, G. P., Andrew, R. M., Canadell, J. G., Ciais, P., Friedlingstein, P., Jotzo, F., van Vuuren, D. P., Le Quéré, C., 2014. Sharing a quota on cumulative carbon emissions. Nature Climate Change Reid, J. S., Reid, E. A., Walker, A., Piketh, S., Cliff, S., Al Mandoos, A., Tsay, S. C., Eck, T. F., 2008. Dynamics of southwest Asian dust particle size characteristics with implications for global dust research, J. Geophys. Res.-Atmospheres 113, D14212, doi: 10.1029/2007JD009752.

Rosenberg, P. D., Parker, D. J., Ryder, C. L., Marsham, J. H., Garcia-Carreras, L., Dorsey, J. R., Brooks, I. M., Dean, A. R., Crosier, J., McQuaid, J. B., and Washington, R., 2014. Quantifying particle size and turbulent scale dependence of dust flux in the Sahara using aircraft measurements, J. Geophys. Res.-Atmospheres 119, 7577-7598.

Schaudt, K. J., Dickinson, R. E., 2000. An approach to deriving roughness length and zero-place displacement height from satellite data, prototyped with BOREAS data. Agricul. Forest Meteorol. 104, 143 – 155.

Schlichting, H., 1936. A wind tunnel study of turbulent flow close to regularly arrayed rough surfaces. Ing.-Arch. NACA Technical Memorandom 823, Vol. 7, pp. 1-34.

Shao, Y., Raupach, M. R., 1992. The overshoot and equilibration of saltation. J. Geophys. Res. 97, 20599-20564.

Shao, Y., Raupach, M. R., Findlater, P. A., 1993. Effect of saltation bombardment on the entrainment of dust by wind. J. Geophys. Res.-Atmospheres 98, 12719-12726.

Shao, Y., Raupach, M. R., Leys, J. F., 1996. A model for predicting aeolian sand drift and dust entrainment on scales from paddock to region. Australian Journal of Soil Research 34, 309-342, 1996.

Shao, Y., Lu, H., 2000. A simple expression for wind erosion threshold friction velocity. J. Geophys. Res. 105, 22437–22443.

Shao, Y., 2001. A model for mineral dust emission. J. Geophys. Res. - Atmospheres 106, 20239-20254.

Shao, Y., 2004. Simplification of a dust emission scheme and comparison with data. J. Geophys. Res. -Atmospheres 109, D10202, doi: 10.1029/2003JD004372.

Shao, Y., 2008. Physics and Modelling of Wind Erosion. Springer Verlag, 452 p.

Shao, Y., Yang, Y., 2008. A theory for drag partition over rough surfaces. J. Geophys. Res. - Earth Surface 113, F02S05, doi: 10.1029/2007JF000791.

Shao, Y., Ishizuka, M., Mikami, M., Leys, J. F., 2011. Parameterization of size-resolved dust emission and validation with measurements. J. Geophys. Res. - Atmospheres 116, D08203, doi: 10.1029/2003JD004372.

Shao, Y., K.-H. Wyrwoll, A. Chappell, J. Huang, Z. Lin, G. McTainsh, M. Mikami, T. Y. Tanaka, X. Wang, and S. C. Yoon, 2011. Dust cycle: An emerging core theme in Earth system science. Aeolian Research 2 (4), 181-204.

Shields, A., 1936. Application of similarity principles and turbulence research to bed-load movement (in German). Preuss. Vers. Anst. Wasserb. Schiffb., No. 26, Berlin.

Shinoda, M., Gillies, J.A., Mikami, M., Shao, Y., 2011. Temperate grasslands as a dust source: Knowledge, uncertainties, and challenges. Aeolian Research 3 (3), 271-293, doi: 10.1016/j.aeolia.2011.07.001.

Sow, M., Alfaro, S. C., Rajot, J. L., Marticorena, B., 2009. Size resolved dust emission fluxes measured in Niger during 3 dust storms of the AMMA experiment. Atmos. Chem. Phys. 9, 3881-3891.

Stallard, R. F., 1998. Terrestrial sedimentation and the carbon cycle: Coupling weathering and erosion to carbon burial. Global Biogeochem. Cy. 12, 231–257.

Steffen, W., 2015. Michael Raupach (1950 – 2015). Nature Climate Change 5, 296, doi: 10.1038/nclimate2591.

Stout, J. E., Zobeck, T. M., 1997. Intermittent saltation. Sedimentology 44, 959-970.

Strong, C.L., Leys, J.F., Raupach, M.R., Bullard, J.E., McTainsh, G.H., Aubault, H.A. (2015) Development and calibration of a micro wind tunnel with application to erosion measurements from rangelands, mine tailings and claypans. Environmental Fluid Mechanics (submitted for review).

Sutton, S. L. F., McKenna-Neuman, C., 2008. Sediment entrainment to the lee of roughness elements: Effects of vortical structures. J. Geophys. Res. - Earth Surface 113, F2, doi: 10.1029/2007JF000783.

Tian, X., Li, Z. Y., van der Tol, C., Su, Z., Li, X., He, Q. S., Bao, Y. F., Chen, E. X. , Li, L. H., 2011. Estimating zero-plane displacement height and aerodynamic roughness length using synthesis of LiDAR and SPOT-5 data. Remote Sensing of Environment 115, 2330 – 2341.

Walter, B., Gromke, C. Lehning, M., 2012a. Shear-stress partitioning in live plant canopies and modifications to Raupach's model. Boundary-Layer Meteorol. 144, 217-241.

Walter, B., Gromke, C., Leonard, K. C., Manes, C., Lehning, M., 2012b. Spatio-temporal surface shear-stress variability in live plant canopies and cube arrays. Boundary-Layer Meteorol. 143, 337-356.

Webb, N.P., Okin G. S., Brown, S., 2014. The effect of roughness elements on wind erosion: The importance of surface shear stress distribution. J. Geophys. Res. – Atmospheres 119 (10), 6066-6084, doi: 10.1002/2014JD021491.

Wiggs, G.F.S., Baird, A. J., Atherton, R. A., 2004: The dynamic effects of moisture on the entrainment and transport of sand by wind. Geomorphology 59 (1-4), 13-30.

Wolfe, S. A., Nickling, W. G., 1996. Shear stress partitioning in sparsely vegetated desert canopies. Earth Surf. Proc. Landforms 21, 607-619.

Wooding, R. A., Bradley, E. F., Marshall, J. K., 1973. Drag due to regular arrays of roughness elements of varying geometry. Boundary-Layer Meteorol. 5, 285 – 308.

Wu, Y., Gong, P., Liu, Q., Chappell, A., 2009. Retrieving photometric properties of desert surfaces in China using the Hapke model and MISR data. Remote Sensing of Environment 113 (1), 213-223, http://dx.doi.org/10.1016/j.rse.2008.09.006.

Yang, Y., Shao, Y., 2005: Drag partition and its possible implications for dust emission. Water, Air and Soil Pollution: Focus 5, 251-259.

Yue, X., Wang, H. J., Liao, H., Fan, K., 2010. Simulation of dust aerosol radiative feedback using the GMOD: 2. Dust-climate interactions. J. Geophys. Res. – Atmospheres 115, D04201.

Zender, C. S., Bian, H. S., Newman, D., 2003. Mineral Dust Entrainment and Deposition (DEAD) model: Description and 1990s dust climatology. J. Geophys. Res. - Atmospheres 108, 4416.

Zhang, L., Kok, J. F., Henze, D. K., Li, Q., Zhao, C., 2013. Improving simulations of fine dust surface concentrations over the western United States by optimizing the particle size distribution. Geophys. Res. Lett. 40, 3270-3275.

Zimon, A.D., 1982. Adhesion of Dust and Powder. Consultants Bureau, New York.

Zobeck, T. M., Gill, T. E., Popham, T. W., 1999. A two-parameter Weibull function to describe airborne dust particle size distributions. Earth Surf. Proc. Landforms 24, 943-955.

Fig. 1. Michael R. Raupach (back, 6th left) among the participants of the 1st Australian Workshop on Wind Erosion, 1991, Murdoch University, Perth. Several contributors to this paper were among the participants: Grant McTainsh (front, 1st left), Paul Findlater (front, 2nd left), Yaping Shao (back, 1st left), William Nickling (back, 5th left), John Leys (back, 7th left). The workshop convener was William Scott (front, 3rd left).

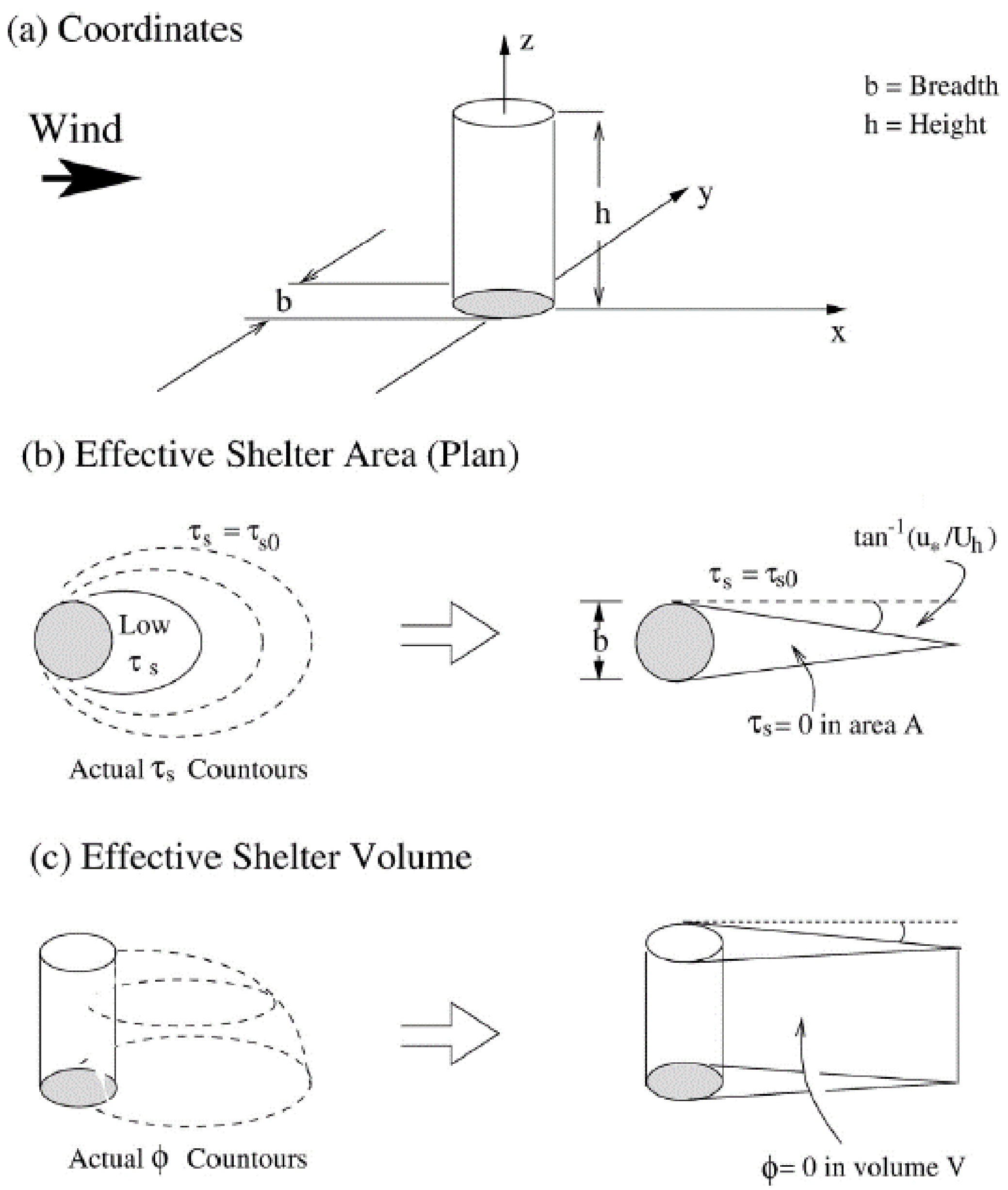

Fig. 2. Raupach's conceptual model for drag partitioning. A rough surface is considered to consist of roughness elements and a substrate surface. A roughness element produces an effective sheltering area and volume. The integrative effect of the roughness elements can be estimated by random superposition [Redrawn from Raupach (1992)].

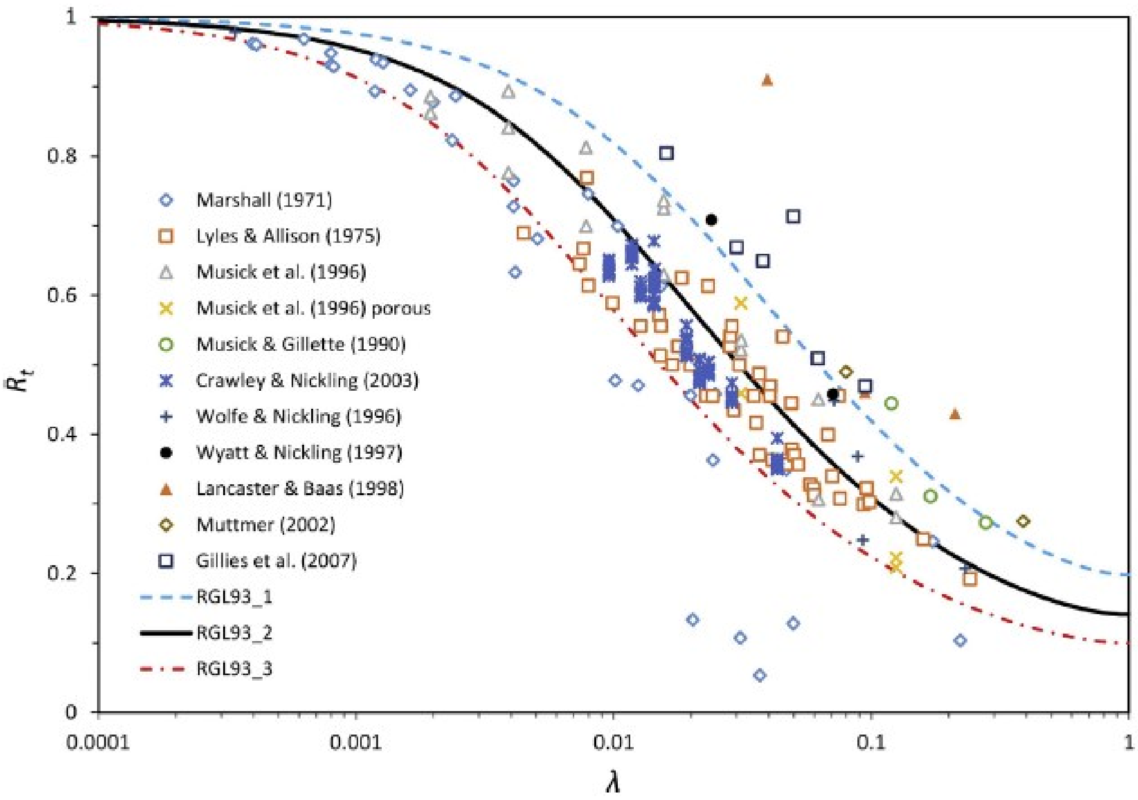

Fig. 3. A compilation of Rt versus k data from wind-tunnel and field experiments (symbols). RGL93_1, RGL93_2 and RGL93_3 are the estimates using the Raupach et al. (1993) scheme with m = 0.5, r = 1, and b = 100, 200 and 400, respectively.

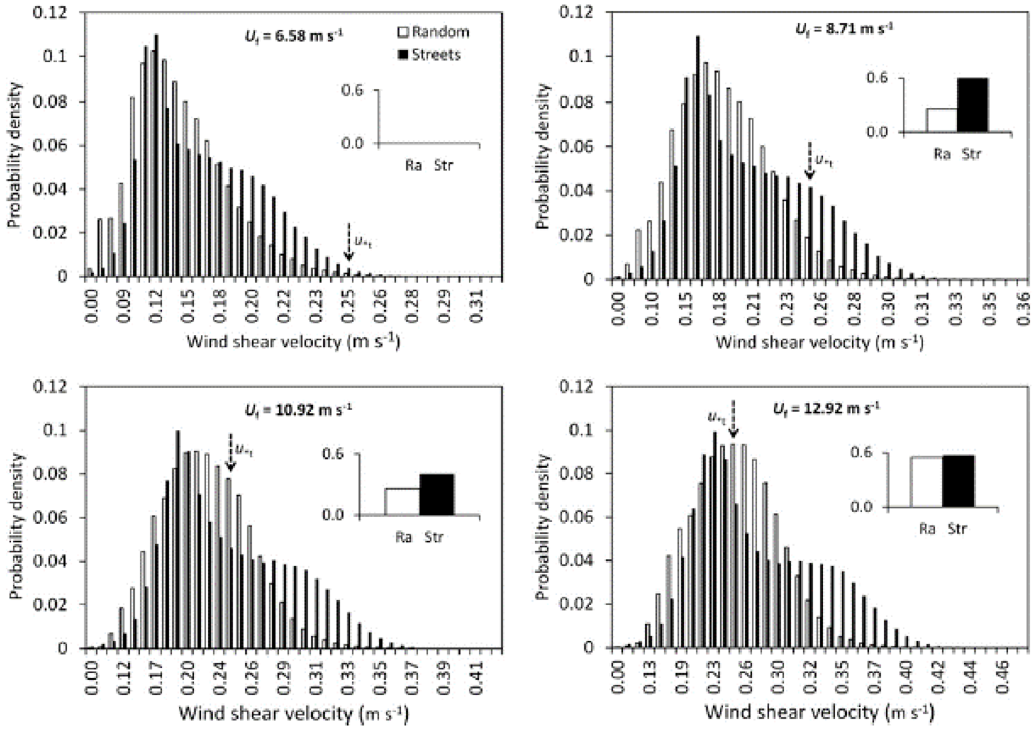

Fig. 4. Histograms illustrating the effect of the 'random' and 'street' roughness configurations on wind shear velocity (u_*) calculated from measured surface shear stress (τ_s) distributions at a roughness density $\lambda = 0.10$ and four free stream wind velocities (U_f). Inset graphs show the proportion of τ_s greater than a threshold shear velocity $u_{*t} = 0.25$ m s^{-1} for the random (Ra) and street (Str) configurations.

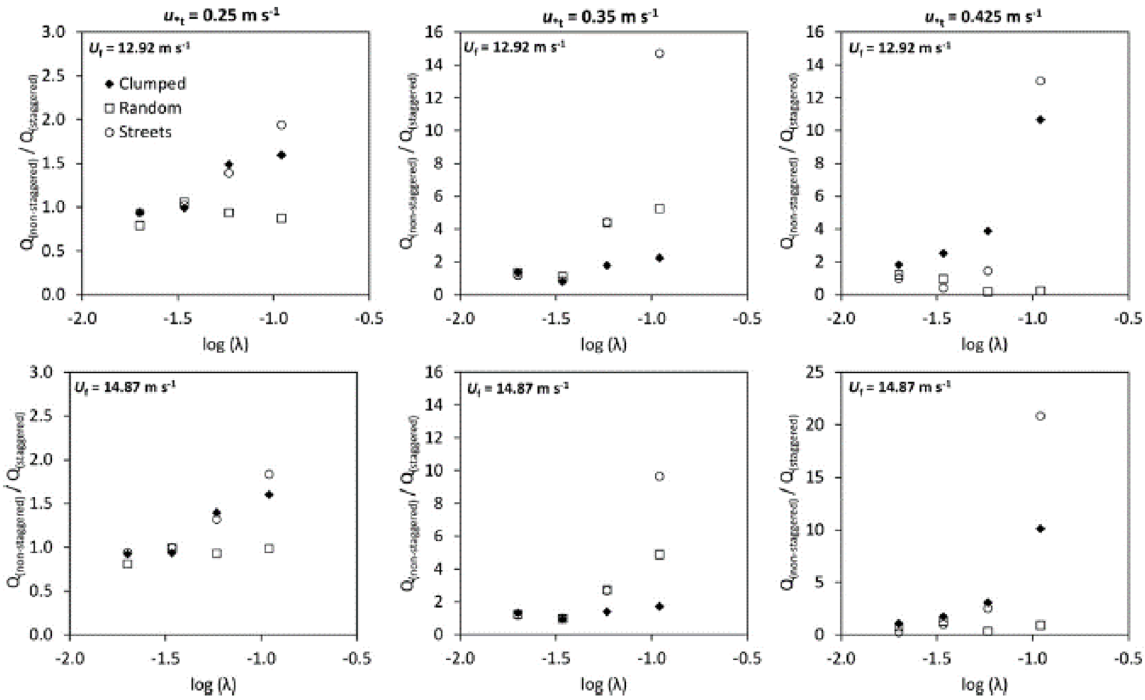

Fig. 5. Graphs showing roughness configuration effects on horizontal sediment mass flux (Q), expressed as the ratio of Q for the ‘clumped’, ‘random’ and ‘street’ configurations relative to Q for the ‘staggered’ configurations at a range of λ and U_f.

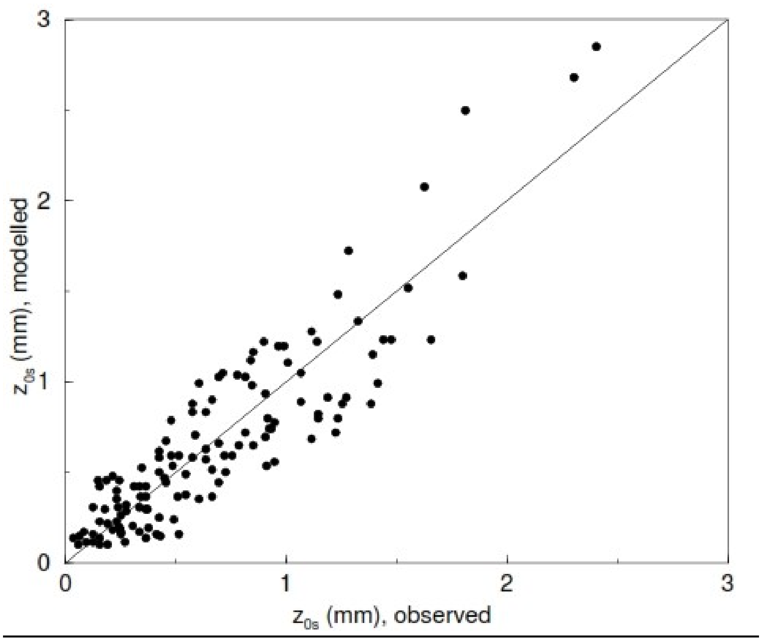

Fig. 6. Modelled saltation roughness length z_{0s} using Equation (20) versus field measurements of Gillette et al. (1998).

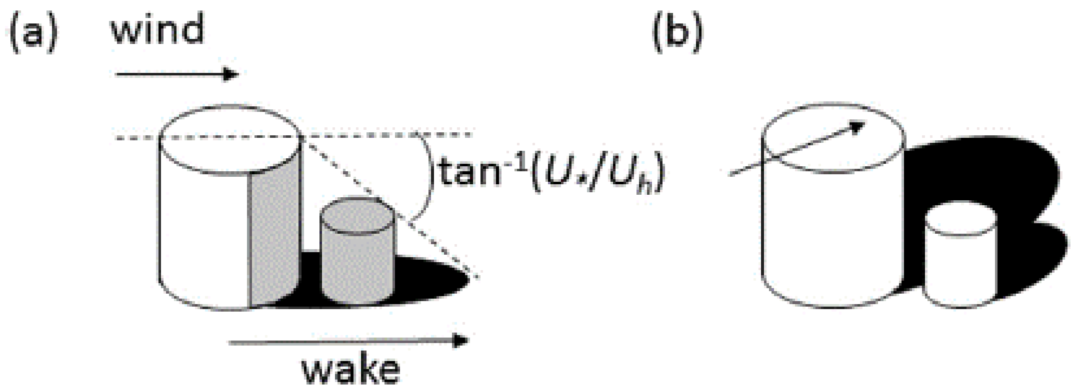

Fig. 7. (a) Roughness elements protect a portion of the substrate surface that may include all or part of other roughness elements in a heterogeneous surface. (b) A change in wind direction redefines the sheltering effect.

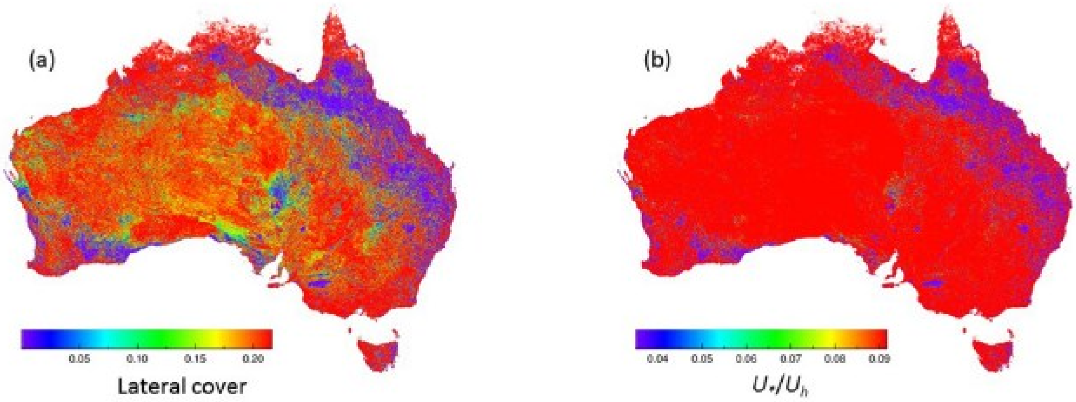

Fig. 8. Examples of aerodynamic properties (a) u_*/Uh and (b) lateral cover estimated from the MODIS MCD43A3 albedo product (500 m resolution) for Australia 1 Jan, 2013.

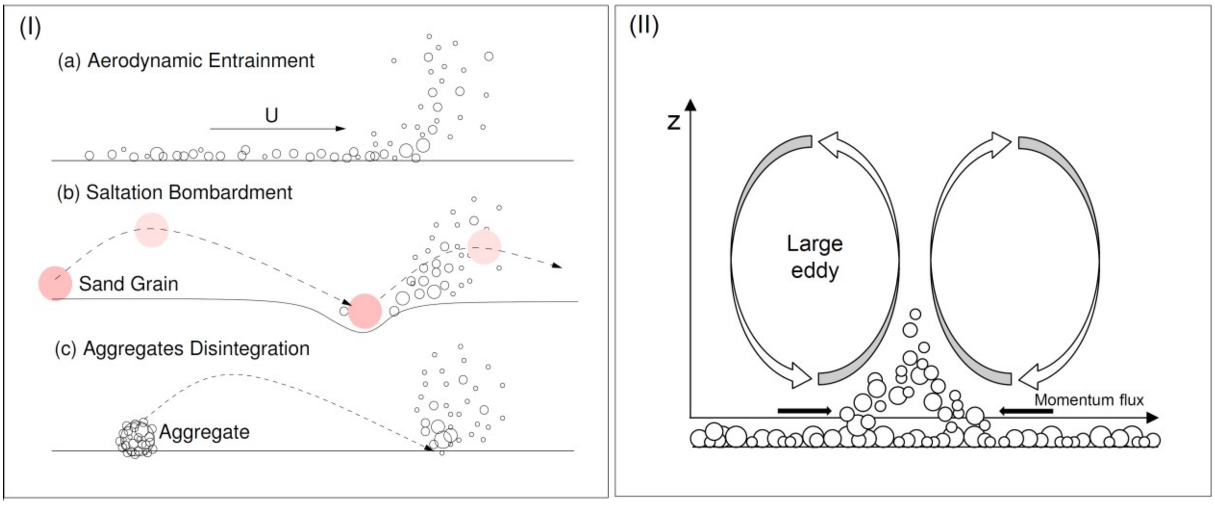

Fig 9. Mechanisms for dust emission. (I) Dust emission by (a) aerodynamic lift, (b) saltation bombardment and (c) aggregate disintegration. Traditionally, these processes are considered to be driven by mean wind shear, but large eddies can also cause intermittent sand drift and dust emission. (II) Illustration of particle lifting caused by the momentum intermittently transported to the surface by turbulent eddies. Saltation may be but does not need to be involved. (I) modified from Shao (2008) and (II) modified from Klose and Shao (2013).

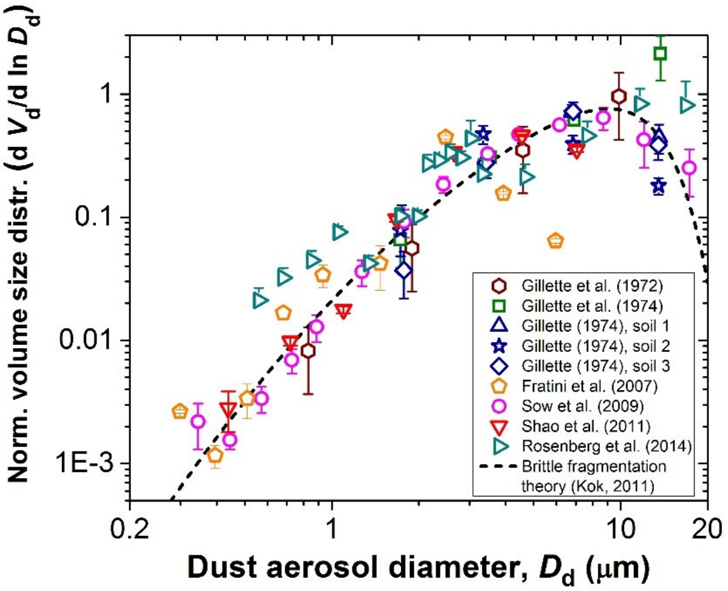

Fig. 10. Compilation of measurements of the volume size distribution of dust aerosols at emission (colored data), compared with the theoretical prediction from brittle fragmentation theory (dashed line). Measurements by Gillette and colleagues (Gillette et al., 1972; Gillette, 1974; Gillette et al., 1974) were taken in Nebraska and Texas and used optical microscopy, whereas measurements by Fratini et al. (2007), Sow et al. (2009), and Shao et al. (2011) used optical particle counters and were respectively taken in China, Niger, and Australia. All these measurements were made on the ground during wind erosion events. In contrast, the measurements of Rosenberg et al. (2014) were made from an airplane flying over the northwestern Sahara, and used high-frequency optical particle counters to obtain the size-resolved dust flux from eddy covariance. All measurements were normalized following the procedure described in Kok (2011b) and Mahowald et al. (2014).

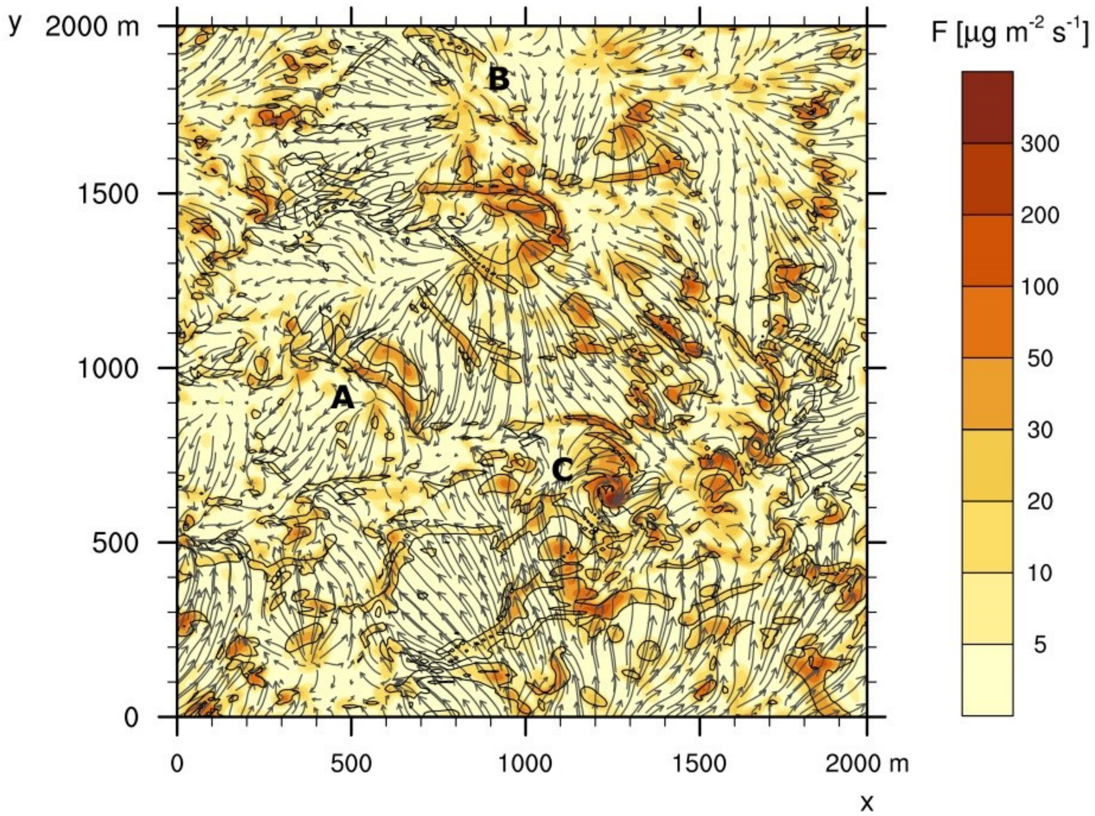

Fig. 11. Turbulent wind speed (vectors, in m s^{-1}) and instantaneous turbulent momentum flux (black contour lines at 1 N m^{-2}) at 10 m height together with turbulent dust emission (shaded, in µg m^{-2} s^{-1}). Updated from Klose and Shao (2013) by inclusion of the dust emission scheme of Klose et al. (2014).

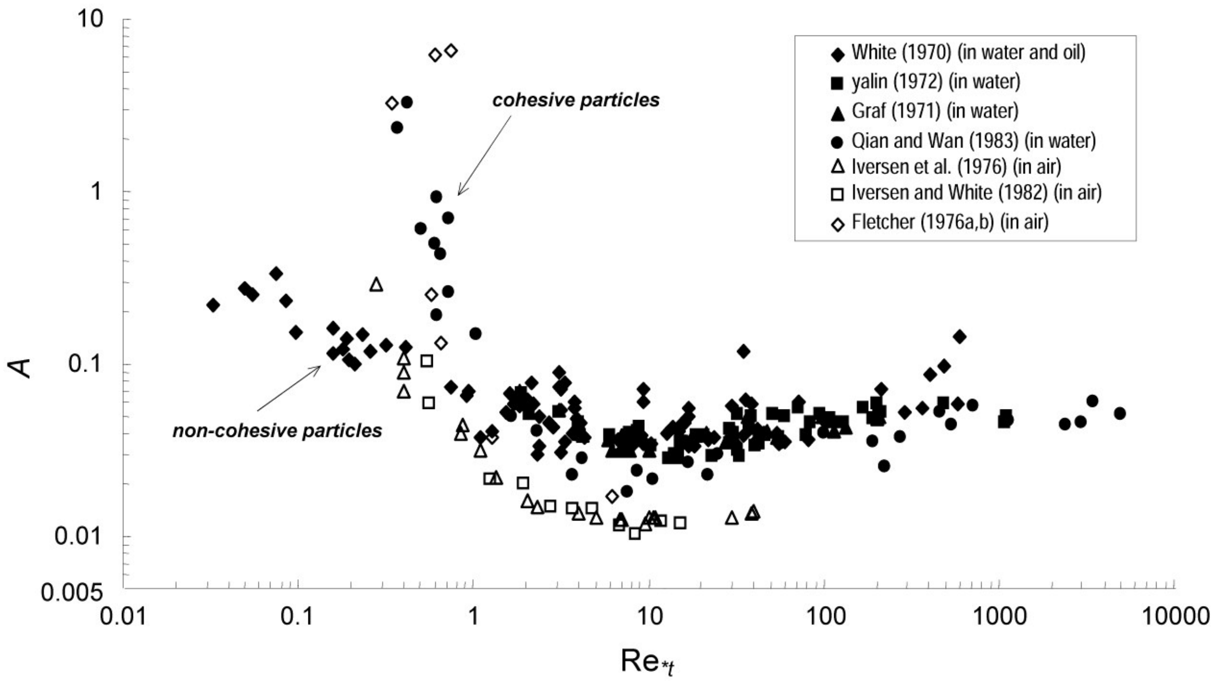

Fig. 12. Dimensionless threshold shear stress A as a function of particle Reynolds number *Re*∗t based on data obtained in water flow (filled) and in air stream (unfilled). These two groups of observations depart both at the large *Re*∗t regime, where aerodynamics dominates and for small *Re*∗t values, where particle cohesion becomes important in determine A. From Lu et al. (2005).